

AEDC-TR-71-13

**ARCHIVE COPY
DO NOT LOAN**



**SOME EXPERIMENTAL TESTS TO CHANGE THE
TOTAL VOLUME AND/OR MOLECULAR WEIGHT
OF ROCKET ENGINE EXHAUST GAS
IN AN ALTITUDE TEST FACILITY**

A. J. Zazzi, J. R. McDowell, and J. W. Hale

ARO, Inc.

March 1971

This document has been approved for public release and sale; its distribution is unlimited.

**ENGINE TEST FACILITY
ARNOLD ENGINEERING DEVELOPMENT CENTER
AIR FORCE SYSTEMS COMMAND
ARNOLD AIR FORCE STATION, TENNESSEE**

PROPERTY OF U. S. AIR FORCE
F40600-1-C-002

AEDC TECHNICAL LIBRARY



5 0720 00033 0003

NOTICES

When U. S. Government drawings specifications, or other data are used for any purpose other than a definitely related Government procurement operation, the Government thereby incurs no responsibility nor any obligation whatsoever, and the fact that the Government may have formulated, furnished, or in any way supplied the said drawings, specifications, or other data, is not to be regarded by implication or otherwise, or in any manner licensing the holder or any other person or corporation, or conveying any rights or permission to manufacture, use, or sell any patented invention that may in any way be related thereto.

Qualified users may obtain copies of this report from the Defense Documentation Center.

References to named commercial products in this report are not to be considered in any sense as an endorsement of the product by the United States Air Force or the Government.

SOME EXPERIMENTAL TESTS TO CHANGE THE
TOTAL VOLUME AND/OR MOLECULAR WEIGHT
OF ROCKET ENGINE EXHAUST GAS
IN AN ALTITUDE TEST FACILITY

A. J. Zazzi, J. R. McDowell, and J. W. Hale
ARO, Inc.

This document has been approved for public release and
sale; its distribution is unlimited.

FOREWORD

The work reported herein was sponsored by the Arnold Engineering Development Center (AEDC), Air Force Systems Command (AFSC), under Program Element 6241003F, Project 7778.

The results of research presented were obtained by ARO, Inc. (a subsidiary of Sverdrup & Parcel and Associates, Inc.), contract operator of AEDC, AFSC, Arnold Air Force Station, Tennessee, under Contract F40600-71-C-0002. The research was conducted in the Propulsion Research Area (R-2C-1) of the Engine Test Facility (ETF) under ARO Project Nos. RW5816, RW5901, and RW5004 between September 1967 and July 1970. The manuscript was submitted for publication on September 29, 1970.

This technical report has been reviewed and is approved.

Charles E. Cisneros
Captain, USAF
Facility Development Division
Directorate of Civil Engineering

Ernest F. Moore
Colonel, USAF
Director of Civil Engineering

ABSTRACT

This investigation was conducted mainly to determine the possibility of burning fuel-rich combustible exhaust gas mixtures by the injection of either gaseous oxygen or gaseous carbon dioxide into the exhaust stream. The burning of the combustibles, especially hydrogen, results in a large volume decrease when the hot gas is cooled. The reaction of the oxygen or carbon dioxide with combustible products (hydrogen rich in this test) was possible, as evidenced by the results of the chemical analysis of the exhaust products. The possibility of generating an electrostatic field along the viscous mixing boundary between two gases was studied using argon, helium, and steam jets at different energy levels. An electrostatic field along the viscous mixing boundary between two gases (one being steam) was produced in an ungrounded installation; even with only a steam jet in an ungrounded installation, an electrostatic field was generated.

CONTENTS

	<u>Page</u>
ABSTRACT	iii
NOMENCLATURE	vii
I. INTRODUCTION	1
II. APPARATUS	
2.1 Rocket Engine.	1
2.2 Test Cell.	2
2.3 Steam Ejector and Straight Diffuser Section	2
2.4 Burner Section	2
2.5 Water Spray Bank	3
2.6 Exhaust Gas Sample Rake	3
2.7 Electrostatic Field Experiment Installation.	3
2.8 Instrumentation	4
III. TEST PROCEDURE	
3.1 Firing	5
3.2 Sampling	5
3.3 Electrostatic Field Experiment Test Procedure	6
IV. RESULTS AND DISCUSSION	
4.1 Oxygen Injection Experiment	8
4.2 Carbon Dioxide Injection Experiment	10
4.3 Electrostatic Field Experiment	12
V. SUMMARY OF RESULTS	14

APPENDIXES

I. ILLUSTRATIONS

Figure

1. Rocket Engine Schematic	17
2. Test Cell Section	18
3. Test Installation Schematic	19
4. Details of Annular Steam Ejector	20
5. Details of Burner Section.	21
6. Schematic of Water Spray Bank at Exit of Burner Section.	22
7. Exhaust Gas Sample Rake	23

<u>Figure</u>	<u>Page</u>
8. Electrostatic Field Experiment Test Installation	
a. With Disc Electrodes	24
b. With Sphere Electrodes	25
c. Coaxial Nozzle with Sphere Electrodes	26
d. Details of Coaxial Nozzle	27
9. Comparison of Theoretical and Actual (Gas Sample) Percent of Free Hydrogen Burned	28
10. Comparison of Theoretical and Actual (Gas Sample) Percent of Water Formed.	29
11. Relation of Percent of Carbon Dioxide Reacted with Ratio of $(\dot{m}_{CO_2})_i / (\dot{m}_{H_2})_{free}$	30
12. The Theoretical Effect of Burning Free Hydrogen with Carbon Dioxide Injection	31
13. Relation of Oxygen Released to the Carbon Dioxide Injected.	32
14. The Actual (Gas Sample) Effect of Burning Free Hydrogen with Carbon Dioxide	33
15. Relation of Carbon Monoxide Remaining in the Exhaust Gas to the Ratio of $(\dot{m}_{CO_2})_i / (\dot{m}_{H_2})_{free}$	34
16. Relation of Carbon Dioxide Remaining in the Exhaust Gas to the Ratio of $(\dot{m}_{CO_2})_i / (\dot{m}_{H_2})_{free}$	35
 II. TABLES	
I. Measurement Accuracy	36
II. Summary of Oxygen Injection Data	37
III. Summary of Carbon Dioxide Injection Data.	38
III. GAS SAMPLE ANALYSIS CALCULATION	42
IV. VENTURI MASS FLOW EQUATION FOR GASEOUS CARBON DIOXIDE	45
V. METHOD OF CALCULATION FOR THE TABULATED DATA	47

NOMENCLATURE

A	Area, in. ²
C _D	Discharge coefficient
d	Diameter, in.
F	Thrust, lbf
g _c	Standard acceleration of gravity, 32.17 ft-lbm/lbf-sec ²
L*	Characteristic length, in.
m	Mass, lbm
\dot{m}	Mass flow rate, lbm/sec
O/F	Oxidizer-to-fuel ratio
p	Pressure, psia
R	Specific gas constant, ft-lbf/lbm-°R
r	Ratio of throat-to-upstream venturi pressure
T	Temperature, °R
V	Volume, in. ³
y _a	Expansion factor
β	Venturi throat-to-pipe diameter ratio
γ	Ratio of specific heats

SUBSCRIPTS

1, 2	Sample bottle and upstream and throat of flow measuring venturi
b	Burner
CO	Carbon monoxide
CO ₂	Carbon dioxide
c	Cell
d	Duct
e	Ejector
ex	Exit

f	Fuel
free	Free
H ₂	Hydrogen
H ₂ O	Water
i	Injection
mix	Mixture
ne	Nozzle exit
O ₂	Oxygen
o	Oxidizer
Rel	Released
r	Rocket
s	Steam or spray water
t	Total

SUPERSCRIPT

*	Nozzle throat
---	---------------

SECTION I INTRODUCTION

A continuing effort is being made to realistically improve the simulated altitude testing capability in current and proposed testing facilities. The objective of this investigation was to provide a technique to improve the performance capability of ground test facilities by eliminating combustible exhaust products from the rocket engine. The feasibility and technique of this physical process have been established, but the application to various combustible gas compositions and the effects on the facility performance must be determined. The elimination of combustible products from the exhaust of rocket engines will (1) provide a means of reducing the total volume of the exhaust products which plant exhaust compressors must pump, thereby improving the plant performance, (2) make more economically feasible the volumetric containment of toxic exhaust products, and (3) make possible the controllable burning of combustibles of rocket engine exhaust gas, thereby reducing explosive hazards in testing facilities.

During altitude propulsion tests, it is sometimes necessary to (1) inbleed air or inert gas into the test cell or ducting to stabilize test cell pressure, and (2) employ the use of a steam ejector to help pump the cell to a lower pressure. Occasionally an unavoidable air leak may develop in the test cell or ducting that would simulate an air jet into the exhaust gases. These jets, whether needed or unintentional, may be directed into the exhaust products which could contain hazardous explosive mixtures. It is questioned as to whether the action of these jets could generate enough stationary electric charge (electrostatic field) to initiate unwanted ignition.

An attempt was made to determine experimentally the feasibility of generating along the viscous mixing boundary between two gases an electrostatic field of sufficient energy to initiate combustion. This investigation was to establish the interaction potential from two different gases flowing at various gas pressures and velocities using different geometrically designed jets.

SECTION II APPARATUS

2.1 ROCKET ENGINE

A 400-lb-thrust rocket engine (Fig. 1, Appendix I) was used during this test. The propellants were gaseous oxygen and gaseous hydrogen.

The engine ignition system consisted of a specially designed water-cooled spark plug with power supplied from a spark coil to achieve instant ignition. The engine was water jacketed to prevent overheating. Specific engine data are as follows:

$F = 400 \text{ lb}_f$	$p_{tr} = 240 \text{ to } 250 \text{ psia}$
$d^* = 1.0 \text{ in.}$	$\dot{m}_f = 0.150 \text{ to } 0.185 \text{ lb/sec}$
$A_{ne}/A^* = 5.2$	$\dot{m}_O = 0.600 \text{ to } 0.645 \text{ lb/sec}$
$L^* = 30 \text{ in.}$	$O/F = 3.2 \text{ to } 4.4$

2.2 TEST CELL

The test cell section (Fig. 2) was fabricated from a nominal 20-in. -diam pipe 12.50 in. long. The upstream end of the test cell was sealed by a flat plate insert which was used to mount the rocket engine. The downstream end was flanged and secured to the steam ejector or straight diffuser as shown in Fig. 3.

2.3 STEAM EJECTOR AND STRAIGHT DIFFUSER SECTION

The steam ejector (Fig. 4) consisted of a converging inlet and an ejector-diffuser having a symmetrically expanding nozzle. The converging inlet was 8 in. in diameter at the entrance and contracted through a 5-deg half-angle for an overall length of 12.5 in. The ejector was fabricated from 8-in. -nominal-diam standard weight pipe 64 in. long and was equipped with a symmetrically expanding nozzle. The ejector had an area ratio A_d/A^* of 10.88 and a throat area of 4.594 in.². The steam ejector was flanged on both ends. The upstream end was secured to the test cell, and the downstream end was secured to the burner section as shown in Fig. 3.

For the portion of this investigation that covers carbon dioxide injection, the steam ejector (Fig. 4) was replaced by an 8-in. -diam straight diffuser 77.19 in. long. A circular manifold was installed 6 in. from each end of the straight diffuser (Fig. 3). Eight equally spaced nozzles directed perpendicular to the centerline were provided in each manifold.

2.4 BURNER SECTION

The inner wall burner section (Fig. 5) was fabricated from a 64-in. length of 20-in. -nominal-diam standard weight pipe. A manifold was

fabricated from 1-in. stainless steel tubing and installed on the upstream end of the burner section. Eight equally spaced 0.120-in. -diam orifices were provided on the manifold for injecting gaseous oxygen at a 45-deg angle downstream and toward the center of the burner section. These orifices were replaced by 0.250-in. orifices for runs HF-19, -20, and -21. The water jacket burner section was fabricated from 24-in. -nominal-diam standard weight pipe. Cooling was accomplished by single-pass water flow. This section was flanged on both ends. The upstream end was secured to the steam ejector, and the downstream end was secured to the R-2C-1 test cell exhaust duct (Fig. 3).

2.5 WATER SPRAY BANK

The water spray bank (Fig. 6) was fabricated from 0.375-in. -diam tubing 8.40 in. long having seven 0.136-in. -diam orifices in each spray bar. Eight spray bars attached to a circular manifold made from 1.0-in. -diam tubing were installed on the spray duct flange at the exit plane of the burner section (Fig. 3).

2.6 EXHAUST GAS SAMPLE RAKE

The exhaust gas sample rake (Fig. 7) was fabricated from 1.0-in. -diam steel tubing, flattened to 0.25 in. thick; 0.125-in. -diam probes 2.0 in. long were located on equal areas in the 60-in. exhaust duct. The gas sampling system consisted of a rake which was located 23 ft from the engine nozzle exit and installed on a horizontal plane for the full diameter of the exhaust ducting as shown in Fig. 3. The probes were positioned in an upstream direction. Three temperature sensing devices were located on the sampling rake to provide a visual temperature surveillance of the gas stream, probes, and rake. The gas sampling system consisted of automatically operated independent valving units for each probe. All sampling lines and valves were maintained at approximately 200°F to prevent condensation from occurring within the gas lines. The gas samples were collected in stainless steel bottles.

2.7 ELECTROSTATIC FIELD EXPERIMENT INSTALLATION

A 7-in. -diam Pyrex[®] spherical chamber equipped with openings in which gas jets, electrodes, pressure gages, and exhaust tubing could be installed (Fig. 8) was used as the test installation for the electrostatic field experiment. In order to minimize outside electrical interference, the chamber was encased in a grounded copper screen, and the entire system was mounted in a screened room.

The vacuum system consisted of a 15-hp vacuum pump with a capability of pumping the test cell down to 40 microns. The pressure in the test cell could be controlled from 40 microns to atmospheric.

2.8 INSTRUMENTATION

The data parameters of primary interest were engine chamber pressure, engine oxidizer flow, engine fuel flow, manifold oxidizer flow, spray water flow, steam flow, cell pressure, diffuser exit pressure, oxidizer temperature, fuel temperature, and steam temperature. All pressures were measured by an electromechanical device incorporating a strain-gage transfer of mechanical pressure on a diaphragm to a Wheatstone bridge output. All temperatures were measured by Chromel[®]-Alumel[®] type thermocouples (Table I, Appendix II). Engine oxygen flow was determined from pressure and temperature upstream of the 0.243-in. -diam venturi. Engine hydrogen flow was determined from the pressure and temperature measured upstream of a 0.281-in. -diam venturi. The injected gaseous oxygen and/or carbon dioxide manifold flow was determined from the pressure and temperature upstream of a 0.340-in. -diam venturi. Steam flow was determined from steam pressure and temperature upstream of a 4.594-in.² steam ejector nozzle throat area. Spray water flow rate was visually displayed on the control console and manually recorded. All pressures and temperatures were recorded on the digital data acquisition system (DDAS) with a maximum deviation of ± 0.22 percent of full scale on 5-mv range and ± 0.075 percent of full scale on 50-mv range or on a DDAS with a maximum deviation of ± 0.35 percent of full scale on all mv ranges. Data were samples four times a second.

Dial pressure gages were used to visually display the cell pressure, gas pressure, and steam supply pressure.

Two different types of electrodes were built to be used in the electrostatic field experiment: (1) circular flat brass plates 2 in. in diameter (Fig. 8a) and (2) aluminum balls 1.75 in. in diameter (Fig. 8b). The electrostatic voltages were monitored with a highly sensitive electrometer on the center-zero ± 50 -v scale. The electrometer accuracy is 2 percent of full scale.

SECTION III PROCEDURE

3.1 FIRING

Steam was introduced into the plenum section and set at 30 psia with the exit pressure set and maintained at approximately 2 psia.

The propellant and oxygen manifold pressures were set by remotely controlled, direct-acting, self-contained gas, dome-loaded, pressure reducing regulators to give desired propellant flow and afterburner (A/B) oxidizer flow. The amount of oxidizer injected was based on the stoichiometric burning of the fuel-rich engine exhaust. The flow rate was set by adjusting the oxidizer supply pressure upstream of the flow-measuring venturi. The venturi was designed to operate in a choked condition, and the flow coefficient was assumed to be 1.0.

Before each test period, the instrumentation systems were calibrated, and the steam, water, and gas sampling systems were prepared for operation. When the pressures were set to give the desired flow rates, the firing sequencer was initiated at a time designated as T - 0 which automatically initiated the events as follows:

T - 0 sec	Automatic firing sequence started
T + 3 sec	Power to spark plug
T + 3.8 sec	Shutdown if no power at spark plug
T + 4.5 sec	Open engine hydrogen valve
T + 5.0 sec	Open engine oxygen valve
T + 14 sec	Open manifold oxidizer valve
T + 24.5 sec	Open sample bottle valve
T + 34.5 sec	Close sample bottle valve
T + 35.5 sec	Close manifold oxidizer valve
T + 36.5 sec	Close engine oxygen and hydrogen valves
T + 37.5 sec	Turn off power to spark plug

When the engine firing was completed, the injector head and manifold were purged with gaseous nitrogen to remove propellants.

3.2 SAMPLING

To determine the degree of burning and/or dissociation that occurred in the exhaust products, gas samples were taken downstream of the reaction area. The samples were obtained at a predetermined time

period in the engine firing sequence as described in Section 3.1. The sampling procedure was automatically initiated at a preset time after the engine parameters reached a steady-state condition and the injected gaseous oxygen and hydrogen reached the desired flow. A sequence timer controlled the valving operation. The lead exhaust gas in the lines was diverted into a vacuum tank and discarded to remove any impurities, such as moisture, residual gases, etc., from the sample lines and to ensure that contaminant-free samples were obtained from each test. The gas was allowed to flow into the vacuum tank until 12 sec of the engine firing cycle remained. During this period, the sample bottles were also being evacuated to ensure that no contaminants remained in the bottle. Then for the next 10 of the remaining 12 sec, the gas was collected in the sample bottles. A sufficient amount of water was injected into the hot gas at the exit end of the burning section (Figs. 3 and 5) during test runs HF-14, -15, -16, and -18 to cool the exhaust gas to a temperature of approximately 500°F, and the sampling lines were maintained at a temperature sufficient to prevent the condensation of steam. The bottles were then sealed and moved to the analysis laboratory. The laboratory analysis was not begun until one or more days later; during this period, the gas samples remained at room temperature. The gas samples were then analyzed by laboratory techniques using a gas chromatography apparatus.

Nitrogen was used to purge the engine and propellant system. Nitrogen from the engine purge was dissipated through the exhaust ducting. Any nitrogen entrained in the sample lines after the engine purge would have been evacuated into the auxiliary vacuum tank and discarded. The engine nitrogen purge was on for 5 to 10 sec and the elapsed time between firings was 5 or more minutes.

3.3 ELECTROSTATIC FIELD EXPERIMENT TEST PROCEDURE

The jets and electrodes were positioned so that the gas streams were tangential to each other and directed between the electrodes (Fig. 8). Both the gap between the electrodes and the impingement angle of the gas jets were adjustable to provide spacing flexibility between the gas jets and electrodes. The test cell was evacuated to the minimum pressure of 40 micron by means of a 15-hp rotary vacuum pump and was determined to be relatively free from leaks by isolating the cell from the pump and checking the rate of rise of cell pressure.

In order to achieve a range of gas velocities, two sets of jets were used. One set had an inside diameter of 1/16 in. and the other 1/8 in. The gas supply to each jet was individually controlled (0 to 35 psia) so

that gas velocities could be varied relative to each other. The pressure in the test cell was controlled by a manually operated valve between the cell and the vacuum header and by the flow rate of the gases from a standard K bottle.

During a portion of the testing phase, the tangential gas jets (Fig. 8b) were replaced with a coaxial nozzle as shown in Fig. 8c. This nozzle was designed to provide an axisymmetric primary stream (1/8-in. -diam) and a coaxial secondary stream (3/8-in. -diam). Argon and helium gases were interchanged in the primary and secondary jets of the coaxial nozzle. The flat plate electrodes were replaced by the spherical electrodes and all gas flow settings were repeated to determine electrostatic field buildup due to electrode geometry. Later in the test when the coaxial nozzle was used, steam was introduced as the primary stream with argon and helium separately introduced as the coaxial secondary stream. This procedure was then reversed with steam as the coaxial secondary jet and the argon and helium gases separately as the primary jet.

SECTION IV RESULTS AND DISCUSSION

The broad objectives of this project were to (1) experimentally investigate the possibility of burning fuel-rich combustible exhaust gas mixtures with either oxygen or carbon dioxide gas injected into the exhaust stream, (2) investigate and evaluate the completeness of the reaction process by sampling and analyzing the residual exhaust products of combustion, and (3) determine experimentally the feasibility of generating an electrostatic field along the viscous mixing boundary between two gases.

Under these broad objectives, the testing experimentations were initiated as follows: Oxygen was injected downstream of the engine ejector-diffuser inlet at values near stoichiometric. The purpose of this was to consume the free hydrogen emitting from the fuel-rich gaseous oxygen-hydrogen engine. Carbon dioxide was injected at two different positions downstream of the engine diffuser inlet to determine the amount of dissociation and burning with the fuel-rich exhaust products from the gaseous oxygen-hydrogen engine.

An effort was made to experimentally investigate those parameters that may be employed as criteria for predicting the stability of unmixed gases to an electrostatic field along the viscous mixing boundary of the gas jets produced by impinging jet injectors or any other technique.

Originally, this investigation was to determine if the ignition of combustible gases was feasible by subsonic, sonic, and supersonic jets at various pressure levels and jet velocities.

4.1 OXYGEN INJECTION EXPERIMENT

The objective of this study was to establish the feasibility of effecting a decrease in the volume flow rate of the combustible gases in the exhaust products from solid- and liquid-propellant rocket systems. The approach used for the experiment was to burn the excess fuel with oxygen injected at the exit plane of the rocket ejector-diffuser.

Although oxygen presents a feasible solution to this problem, it also presents a potential hazard should the stoichiometric mixture of oxygen-hydrogen fail to ignite and burn completely in the designated area of the test facility. The potential hazard of an oxygen-hydrogen-vapor mixture becomes even more critical because of the wide limits of flammability for hydrogen in an oxygen environment which ranges from a low of 4.65 to a high of 93.9 percent by volume.

Six gas samples were obtained for each test run, although the sampling rake contained 12 probes. However, the six probes used were located on equal area across the entire diameter of the exhaust duct. The effective sampling area was the same for each set of six probes.

Temperature observed by visual readout equipment from thermocouple No. 2 (Nos. 3, 4, and 5 were on DDAS) located in the burner section (Fig. 5) indicated a sharp temperature increase ($\sim 2000^\circ\text{F}$) when oxygen was injected, indicating burning. The temperature indicated by the temperature probes can be 30 to 40 percent low because the probes were immersed only 4 in. into a nominal 20-in.-diam exhaust stream and also because the burner section wall was water cooled, thus reducing the temperature of the gas along the wall area. Attempts were made to use 12-in. temperature probes, but because of the excess temperature and high exhaust stream velocity, the thermocouple would bend downstream in the flow direction so that the temperature indicated was approximately 2 to 3 in. from the burner section wall. The 4-in. thermocouple did resist damage but did not indicate the core temperature of the exhaust stream.

The data in Fig. 9 show both the theoretical (upper curve) and actual data in percent of free hydrogen burned as a function of the ratio of the injected oxygen to free hydrogen which is equivalent to the O/F ratio in the burner section.

The percent of excess hydrogen was obtained by determining the amount of free hydrogen (theoretical amount of excess hydrogen by assuming 100-percent combustion efficiency) that the rocket engine discharged. To this amount of hydrogen was added a quantity of oxygen to bring the gas mixture up to some value near stoichiometric; however, stoichiometric mixtures were not always obtained as shown by the upper curve in Fig. 9.

The lower curve (Fig. 9) shows the percent of hydrogen burned which was obtained from the reaction of known values of free hydrogen and the injected oxygen. The percent of hydrogen burned equals the amount of free hydrogen minus the amount of unburned hydrogen obtained from the exhaust gas samples divided by the amount of free hydrogen. The results of this analysis indicated that the actual amount of free hydrogen burned was about 30 to 35 percent. Each value as indicated in Fig. 9 represents the average of the six gas samples taken across the diameter of the exhaust duct. The distribution of the actual data can be attributed to the sampling technique and sampling analysis of extremely small quantities of hydrogen in the exhaust gas of which approximately 98 percent of the sample was water vapor.

Figure 10 shows the theoretical and actual data results in percent of water formed from the combustion process of an oxygen and hydrogen system versus the ratio of oxygen (rocket engine plus manifold) and free hydrogen $(O/F)_t$ from the rocket engine. Both the theoretical and measured percent of water formed were determined from quantities approaching stoichiometric values for the various rocket engine O/F ratios tested.

The percent of water formed, represented by the test data (Fig. 10), was obtained under the following test conditions and with conditions as indicated in Table II. Condition A represents values from both the theoretical and the sample analysis data which were obtained from the rocket engine exhaust plus the injected oxygen (no steam and no water were added). Condition B (test number HF-19, Table II) includes the same conditions listed under condition A plus the added steam used to drive the steam ejector (test numbers HF-20 and -21). Condition C represents values which were obtained during operation of the rocket engine, the steam ejector, and the cooling sprays (no oxygen was injected, Table II).

Because of the limited O/F range of rocket engine operation, the distribution of the percent of water formed was somewhat restricted; however, the agreement between the theoretical and the measured data was exceptionally good. The amount of water produced by combustion in this series of tests was very small because of the small flow rates of

hydrogen and oxygen. To illustrate this, in test number HF-16 from Table II, the percent of water formed (data points 3 and 5, with oxygen injected, and data points 2 and 4, without oxygen injected) from the combustion of injected oxygen and free hydrogen increased the water content of the exhaust gas by approximately 5 percent.

In condition A, the percent of water produced from the combustion process was without steam and water added to the exhaust stream. All the test runs in this series were fired with a total O/F ratio (includes engine and manifold) slightly below stoichiometric, which resulted in all the oxygen being consumed and a small amount of hydrogen remaining.

4.2 CARBON DIOXIDE INJECTION EXPERIMENT

One procedure used to reduce the explosive potential of the combustible gases in an exhaust system and to increase the density of the mixture to enhance exhaust compressor performance has been to inject a large quantity of inert gas (nitrogen) into the exhaust ducting during the engine firing sequence. This, however, increases the exhauster equipment pumping load and/or the volume of the containment vessel required for toxic exhaust products. These methods of achieving a safe operational procedure are prohibitive in cost and imposed limits on maximum test altitude and/or test duration.

In a continuing effort to improve the altitude testing simulation capabilities in testing facilities, a study was undertaken to investigate compatible gases that might be injected into the exhaust products to initiate the secondary burning of hydrogen.

Theoretical calculations were made to determine whether carbon dioxide injected into the high temperature exhaust gas would dissociate and release oxygen for burning of the excess fuel component. The results of the calculations indicated that dissociation would occur; therefore, a pilot scale feasibility effort was initiated. Because of the limited time available for this effort, the test setup used for the oxygen injection study was modified and used in this investigation.

The number of gas samples obtained from each test run was varied from two to seven. Table III shows the number of samples taken and the probe numbers used during each test run.

Figure 7 identifies the probe position on the sampling rake. Each point on the plotted data represents an analysis of a gas sample for one probe position. There were occasions when either the sample, the

chemical analysis, or both, appeared to be out-of-line and this scatter reduced the effectiveness of the data. A part of the scatter can also be attributed to the limited number of samples per run.

The amount of carbon dioxide injected into the rocket engine exhaust gas was varied $[(\dot{m}_{\text{CO}_2})_i / (\dot{m}_{\text{H}_2})_{\text{free}}$ from 7.2 to 29.2] to determine from the reaction the degree of dissociation of the carbon dioxide and the percent reaction of the free hydrogen as a function of the amount of carbon dioxide injected. The amount of free (unburned) hydrogen was relatively constant for a given O/F ratio.

Carbon dioxide was injected at two locations in an effort to determine if the higher level of temperature near the engine would effect an increase in the amount and/or the rate of dissociation (stations A and B, Fig. 3). At each location, a circular manifold was used with eight equally spaced nozzles (0.250-in. -diam) injecting the carbon dioxide into the rocket engine exhaust stream. At station A, the carbon dioxide gas was injected in a downstream direction at a 45-deg angle to the center of the duct, while at station B, it was injected perpendicular to the exhaust stream. No mechanical devices or flame holders were used to assist in the mixing process.

The results presented in Fig. 11 show the percent of dissociated carbon dioxide versus the ratio of the total flow rate of the carbon dioxide to the flow rate of free or unburned hydrogen in the fuel-rich engine exhaust gas, $(\dot{m}_{\text{CO}_2})_i / (\dot{m}_{\text{H}_2})_{\text{free}}$.

The ratio of the mass flow of carbon dioxide to the mass flow of free hydrogen versus the theoretical percent of hydrogen burned is presented in Fig. 12. The theoretical percent of hydrogen burned was based on burning the oxygen liberated by the carbon dioxide (see Appendixes III, IV, and V for methods of calculation).

The mass flow rate of oxygen released versus the mass flow rate of carbon dioxide injected is presented in Fig. 13.

The percent of free hydrogen burned versus $(\dot{m}_{\text{CO}_2})_i / (\dot{m}_{\text{H}_2})_{\text{free}}$ is presented in Fig. 14. There is a large degree of scatter in the data which is attributed to the inaccuracy of the sample analysis of the hydrogen. The principal contributing factor for this inaccuracy was the extremely small amount of hydrogen (10 percent by weight) in the sample compared with approximately 90 percent of water by weight. This left even smaller quantities of hydrogen, carbon monoxide, and the remaining

unreacted carbon dioxide in the sample from which to obtain a complete analysis (the water, liquid and vapor, was extracted from the sample prior to analysis). Although the data scattered over a range of 6 to 100 percent, it does substantiate the fact that a portion of the carbon dioxide dissociated producing oxygen and carbon monoxide and that a portion of the free hydrogen was burned.

The amount of carbon monoxide produced from the dissociated carbon dioxide indicated that, as the mass rate of carbon dioxide was increased, the temperature of the exhaust gas decreased and the amount of carbon monoxide remaining tended to level off (Figs. 15 and 16). The upstream relative to the downstream injection point for the carbon dioxide shows little if any difference in injection location in producing carbon monoxide.

During test number CO₂-7, steam and water were injected downstream of the carbon dioxide injection point to determine if any of the carbon monoxide would combine with the oxygen in the water and liberate hydrogen as in the water gas reaction. The results of this test compared with tests without water or steam indicate that the water-gas reaction did not occur to a significant degree (Table II).

4.3 ELECTROSTATIC FIELD EXPERIMENT

During altitude propulsion simulation testing, it is sometimes necessary to inbleed either air or an inert gas to stabilize the cell pressure. Occasionally, an unavoidable air leak may develop in the test cell or the exhaust ducting that would simulate an air jet impinging on the exhaust stream. These jets containing oxygen directed into the exhaust products which sometimes contained fuel might generate a static charge of sufficient energy to initiate ignition and result in an explosion.

A model test rig (Fig. 8) was set up for this investigation. A series of tests was conducted at a minimum test chamber vacuum pressure of 40 microns with argon as the lead gas supplied at 5-, 10-, 20-, and 30-psig levels. At each of these pressures, helium was injected from the secondary jet by gradually increasing the helium supply pressure from 0 to 30 psia. During this pressure transition, there was no evidence of any electrostatic field buildup when using the tangential or the coaxial jets (Fig. 8). This same procedure was repeated with helium (lead gas) and argon, and still no electrostatic field buildup was observed. The impingement angle of the tangential jet was changed as was the gap between the electrodes with no success. The above series

was repeated with increased test chamber pressure at different pressure increments up to atmospheric with no indication of electrostatic field buildup. Both gases were started simultaneously at several pressure levels, but no charge was generated.

The next series of tests was run using argon and steam and helium and steam with the coaxial nozzle. The steam was supplied at 18 to 20 psig. The same test parameters and program used for the argon-helium series were repeated for these tests.

When only the argon or helium gas was flowing, there was no indication of any electrostatic field buildup; however, the instant that the steam started flowing an electrostatic field in excess of 50 v was detected between the nozzle and either of the spherical electrodes. The maximum voltage was not determined because 50 v were the maximum for the scale used.

With the argon and steam continuing to flow, an electrical short was placed between the electrode and the nozzle, and the electrostatic field potential difference became zero; however, the instant the shorting bar was removed, an electrostatic field buildup was recorded. When the steam was shut off and the argon continued flowing, the electrostatic field was not indicated; however, with only the steam flowing, there was an electrostatic field indicated. The above procedure was repeated after interchanging the gas and steam jets of the coaxial nozzle. The results were that interchanging of the gas and steam jets did not affect the test results.

Changing the steam from the primary to the secondary coaxial nozzle or changing from the flat plate to the spherical electrode configuration had no effect on the test results.

SECTION V SUMMARY OF RESULTS

An investigation was conducted (1) to experimentally investigate the possibility of burning fuel-rich combustible exhaust gas mixtures by the injection of either oxygen or carbon dioxide gas into the exhaust stream, and (2) to determine experimentally the feasibility of generating an electrostatic field along the viscous mixing boundary between two gases of such magnitude as to propagate ignition. Significant results of the investigation are summarized as follows:

1. The exhaust gas from propulsion systems which contain combustible products such as hydrogen can be burned effectively under typical operating conditions with injected oxygen or carbon dioxide to reduce the volumetric pumping or containment requirement for altitude test facilities.
2. An electrostatic field was produced along the viscous mixing boundary between steam and argon or helium in an ungrounded installation. An electrostatic field was produced by only a steam jet in an ungrounded installation.

APPENDIXES

- I. ILLUSTRATIONS**
- II. TABLES**
- III. GAS SAMPLE ANALYSIS CALCULATION**
- IV. METHOD OF CALCULATION
FOR THE TABULATED DATA**

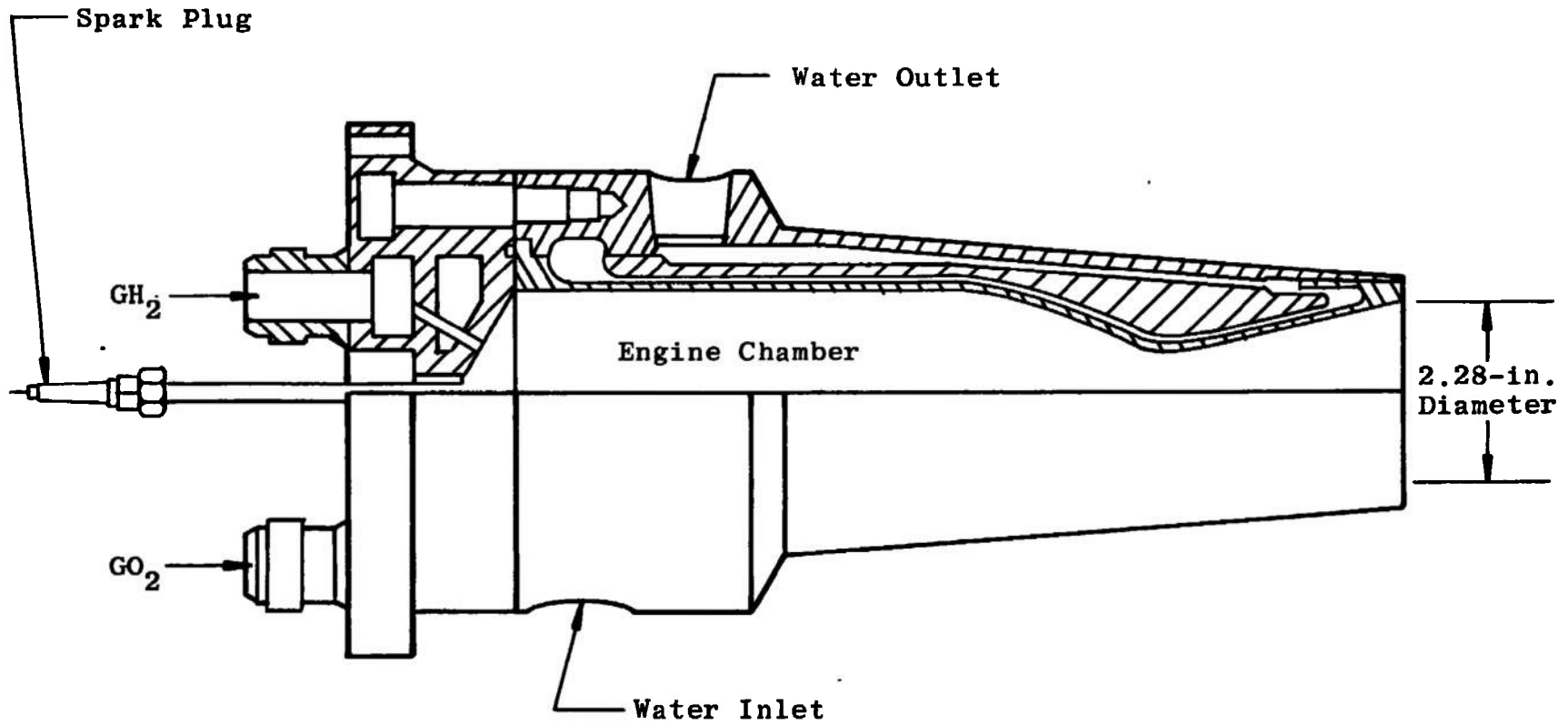


Fig. 1 Rocket Engine Schematic

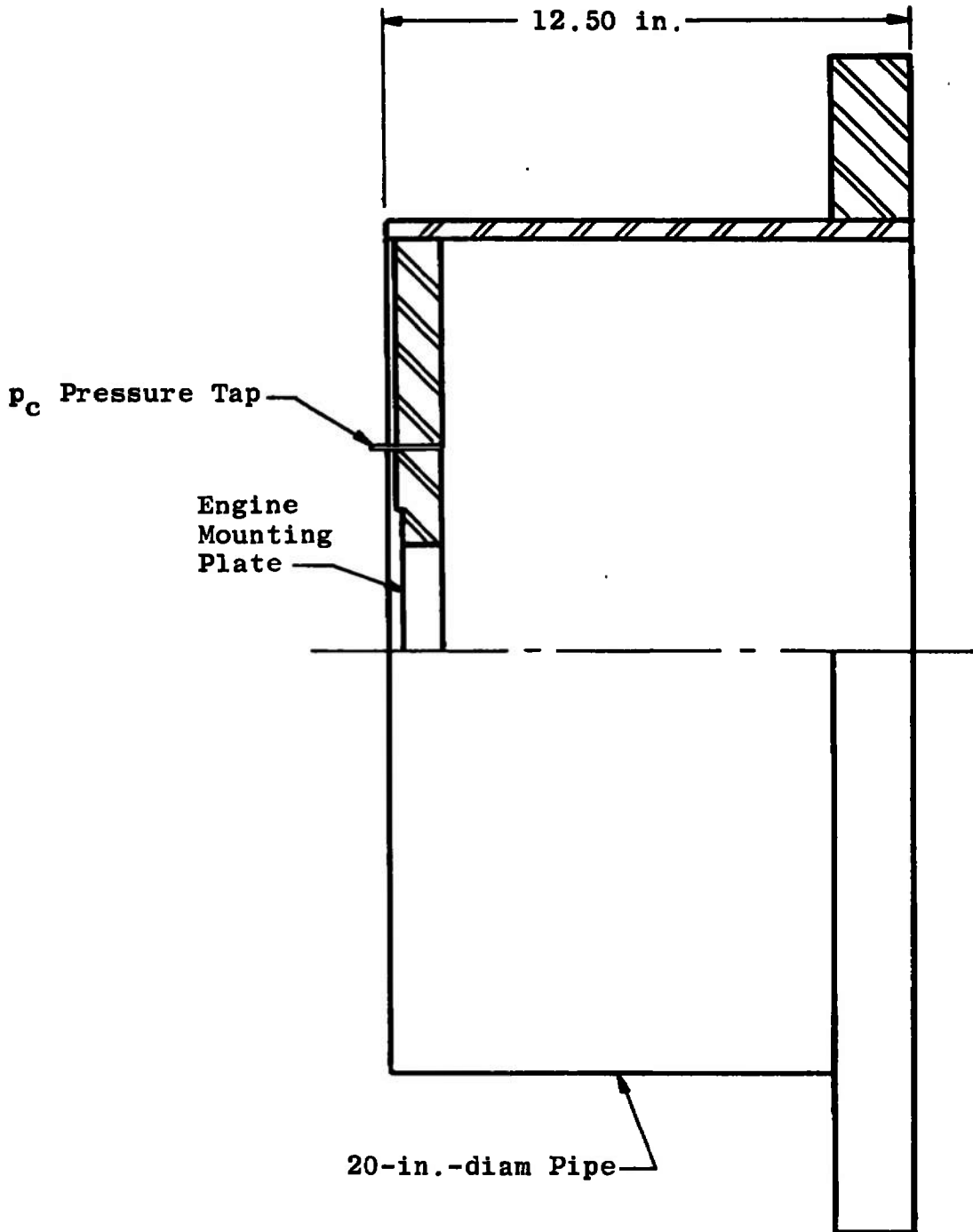
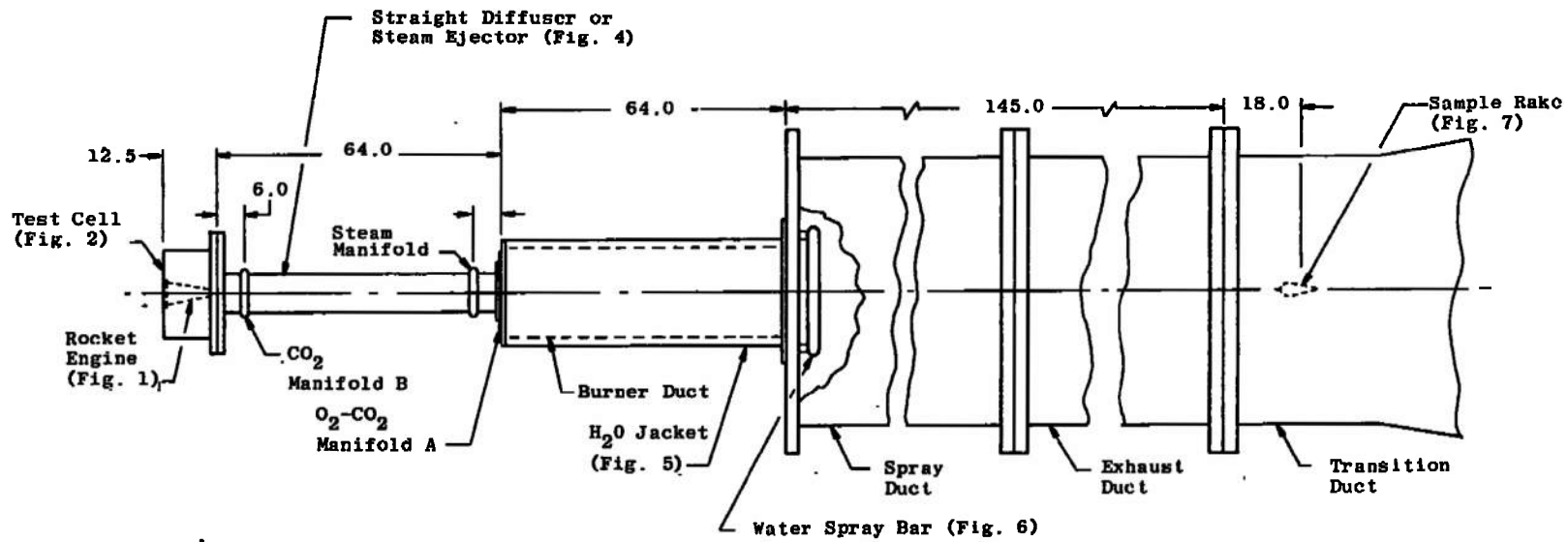
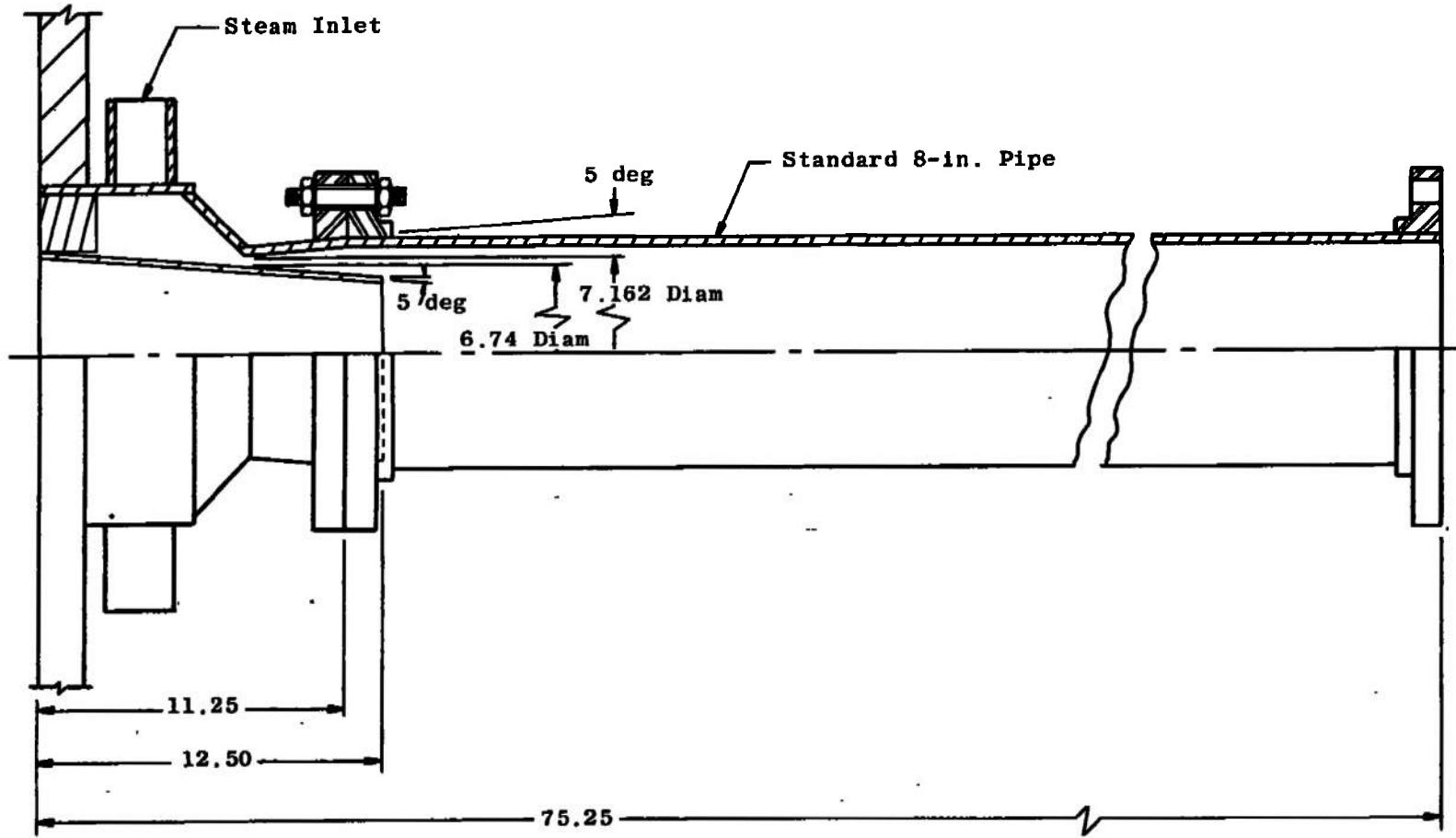


Fig. 2 Test Cell Section



All Dimensions in Inches

Fig. 3 Test Installation Schematic



All Dimensions in Inches

Fig. 4 Details of Annular Steam Ejector

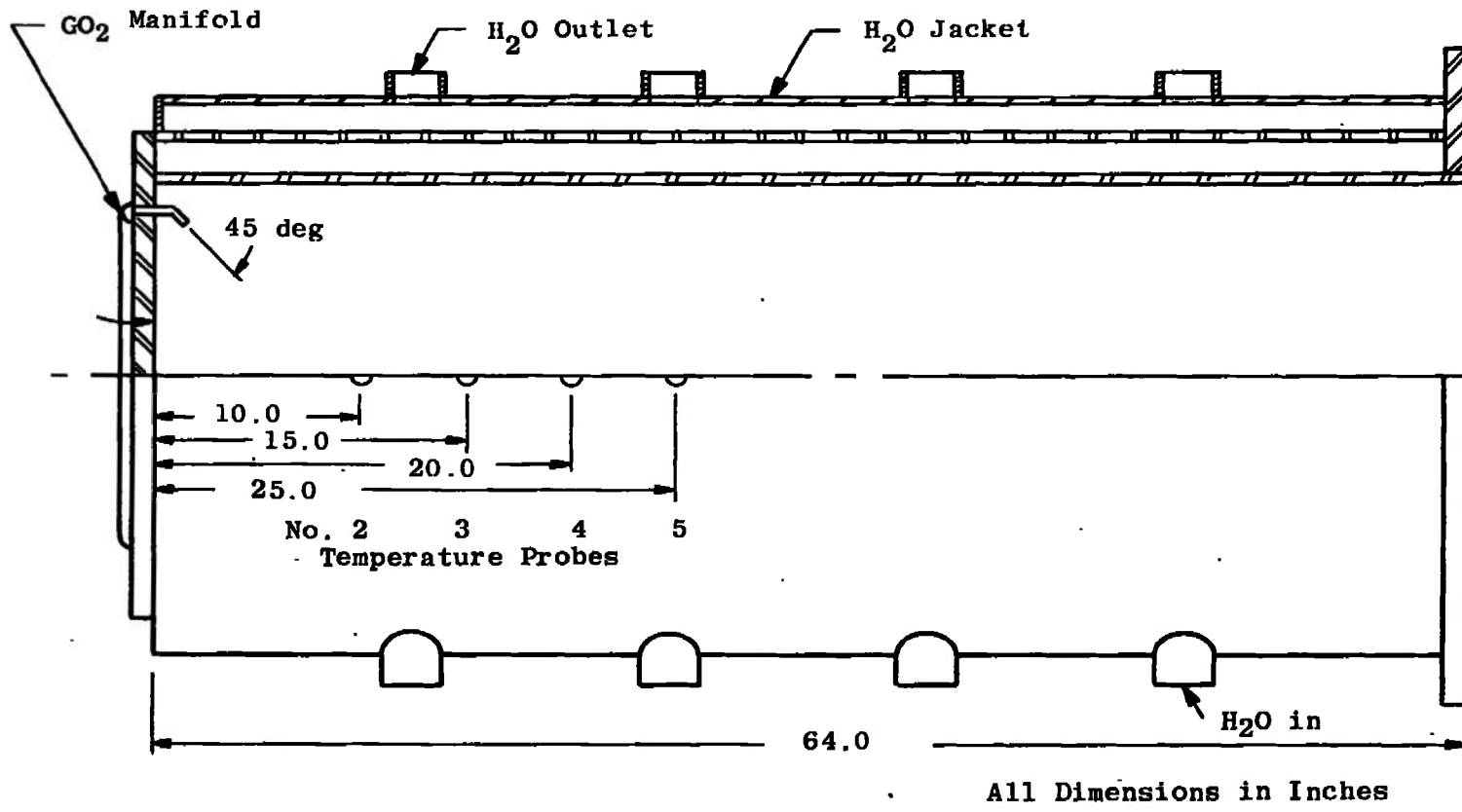


Fig. 5 Details of Burner Section

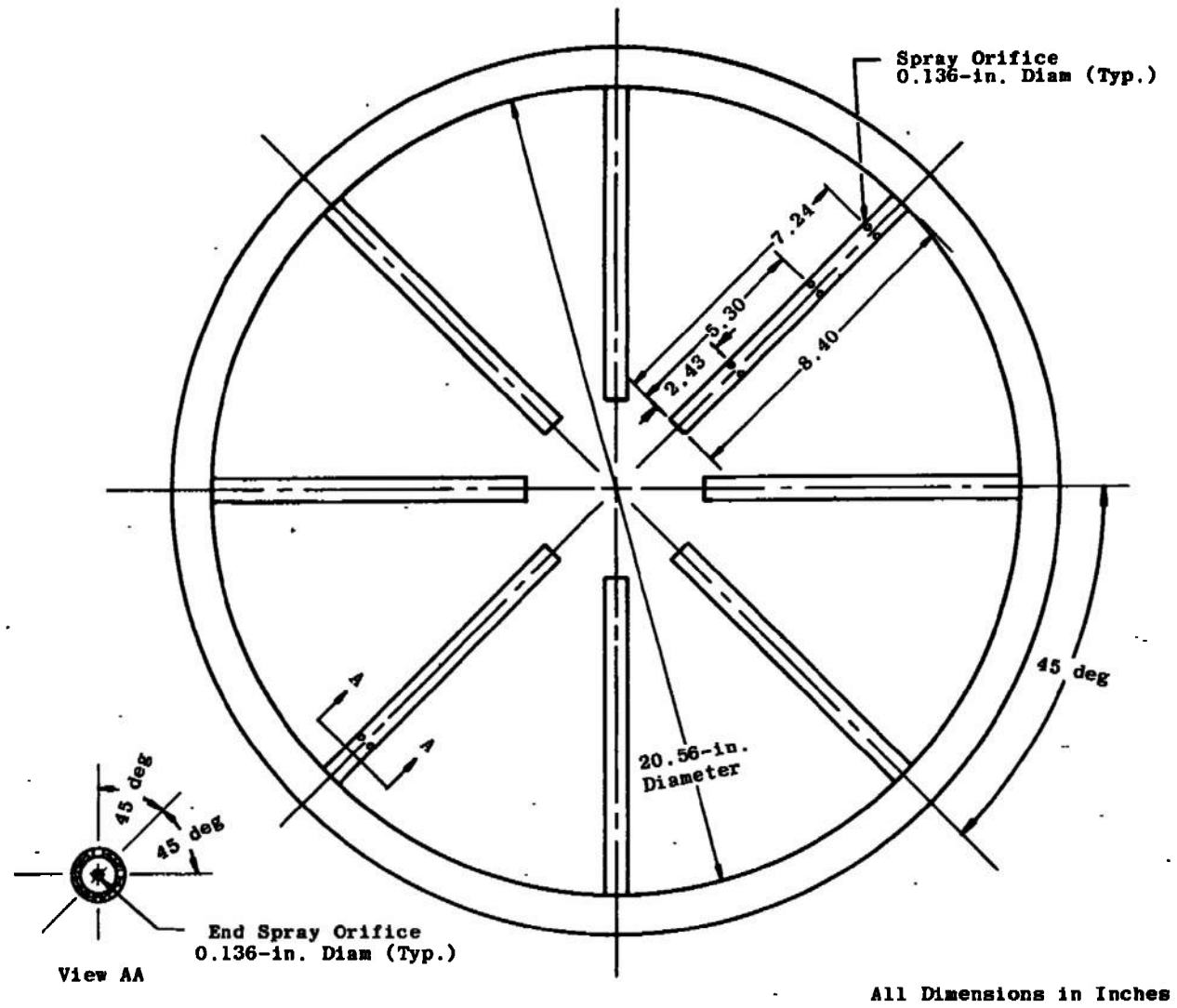


Fig. 6 Schematic of Water Spray Bank at Exit of Burner Section

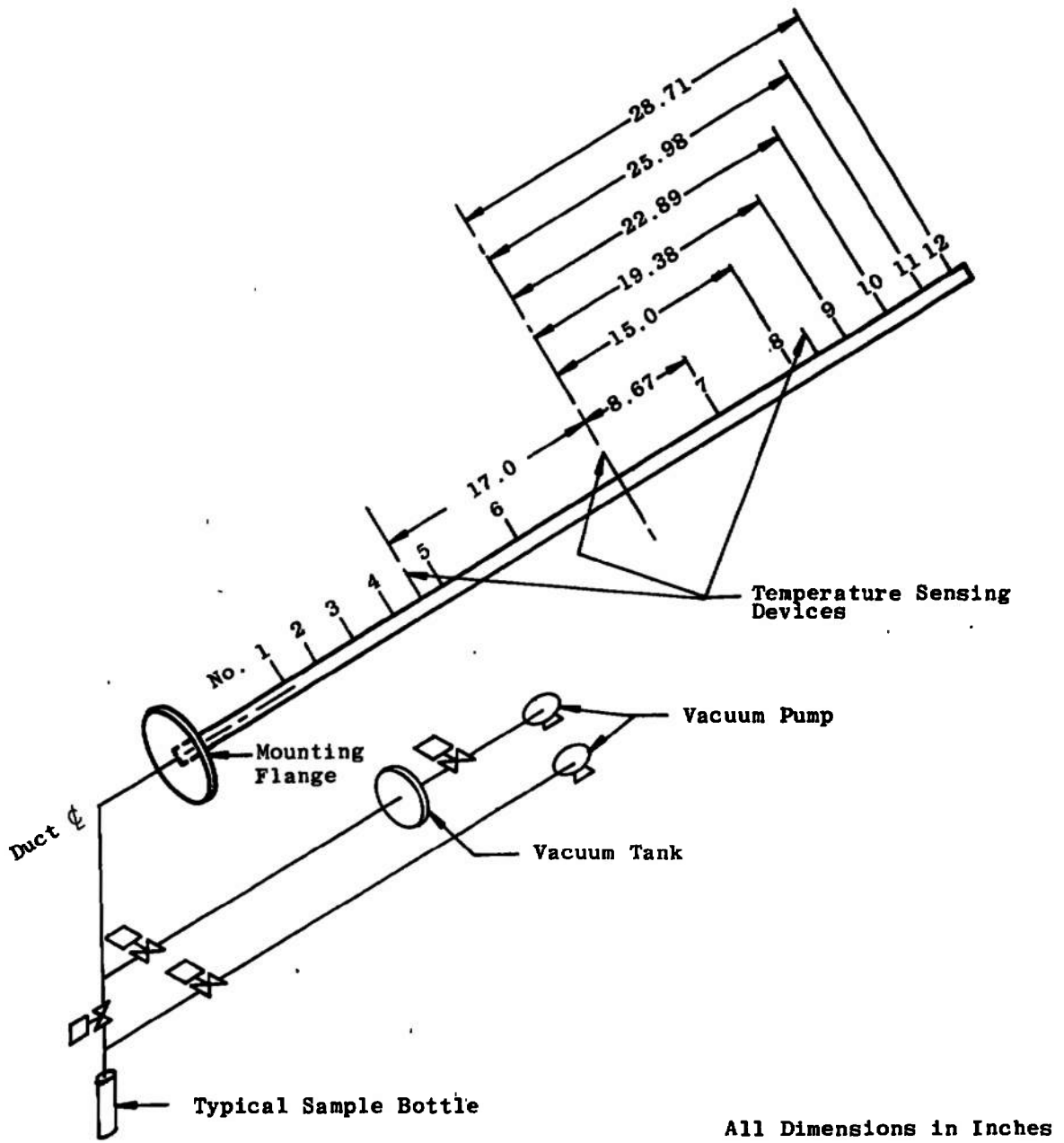
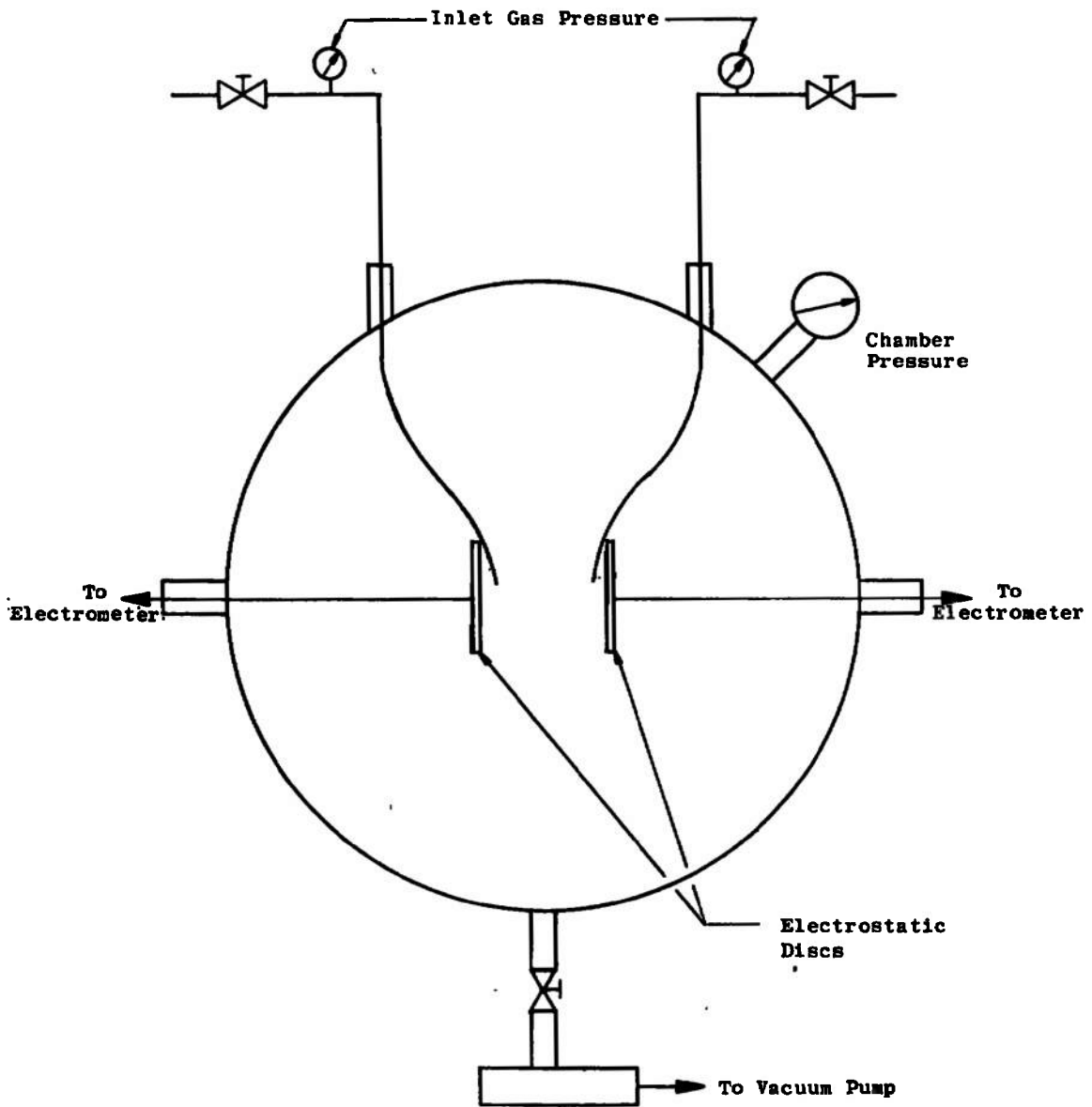
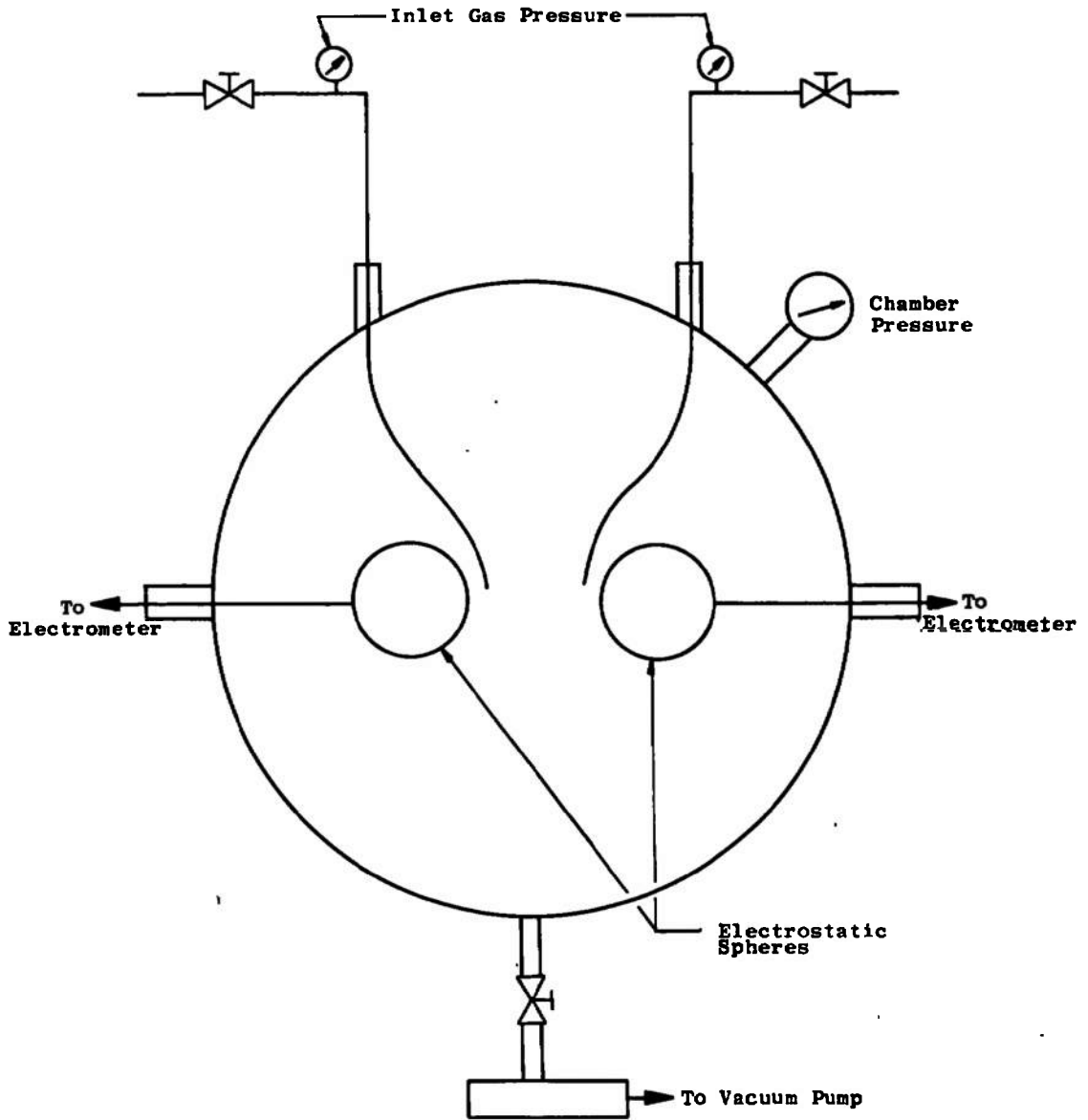


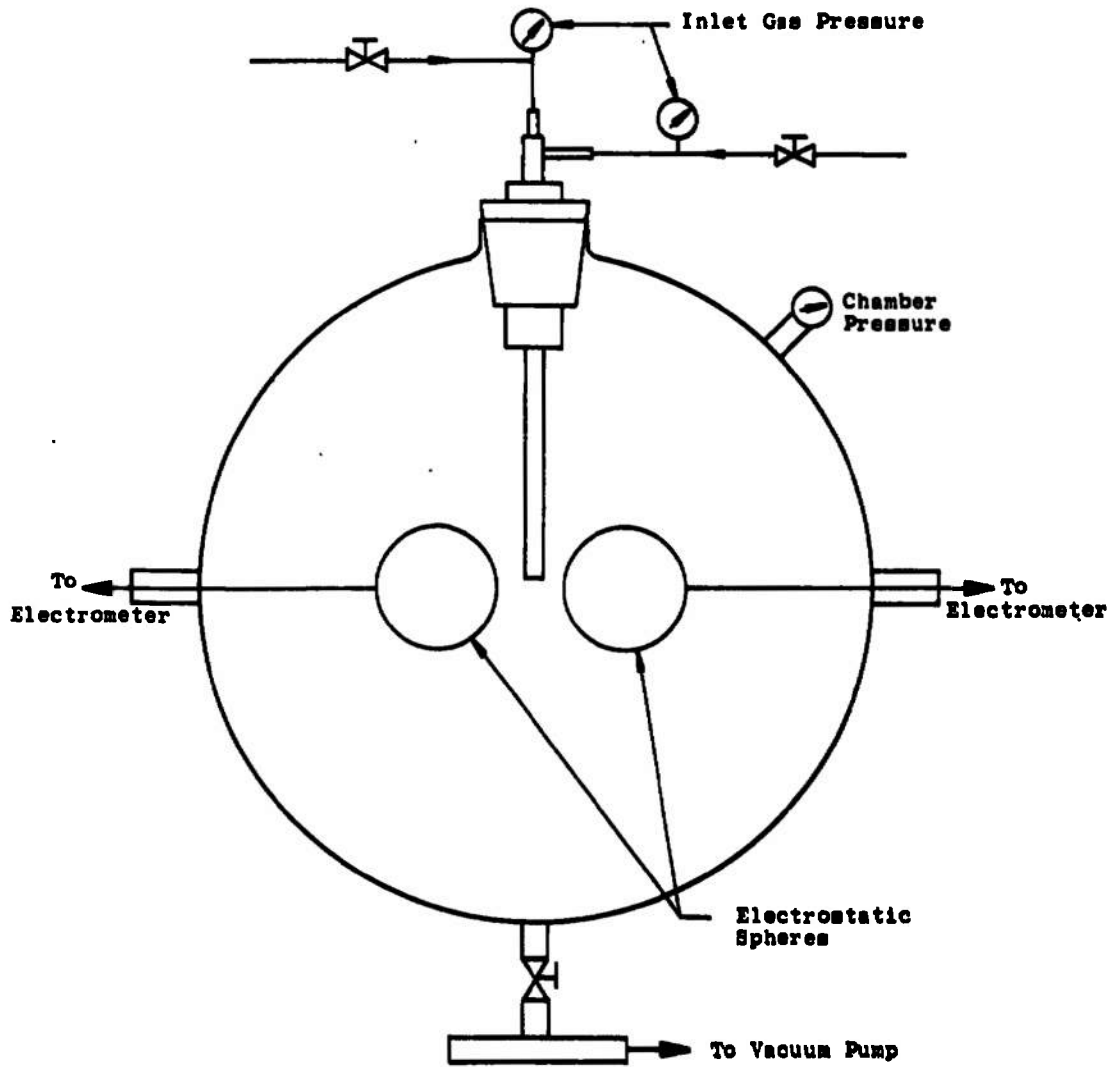
Fig. 7 Exhaust Gas Sample Rake



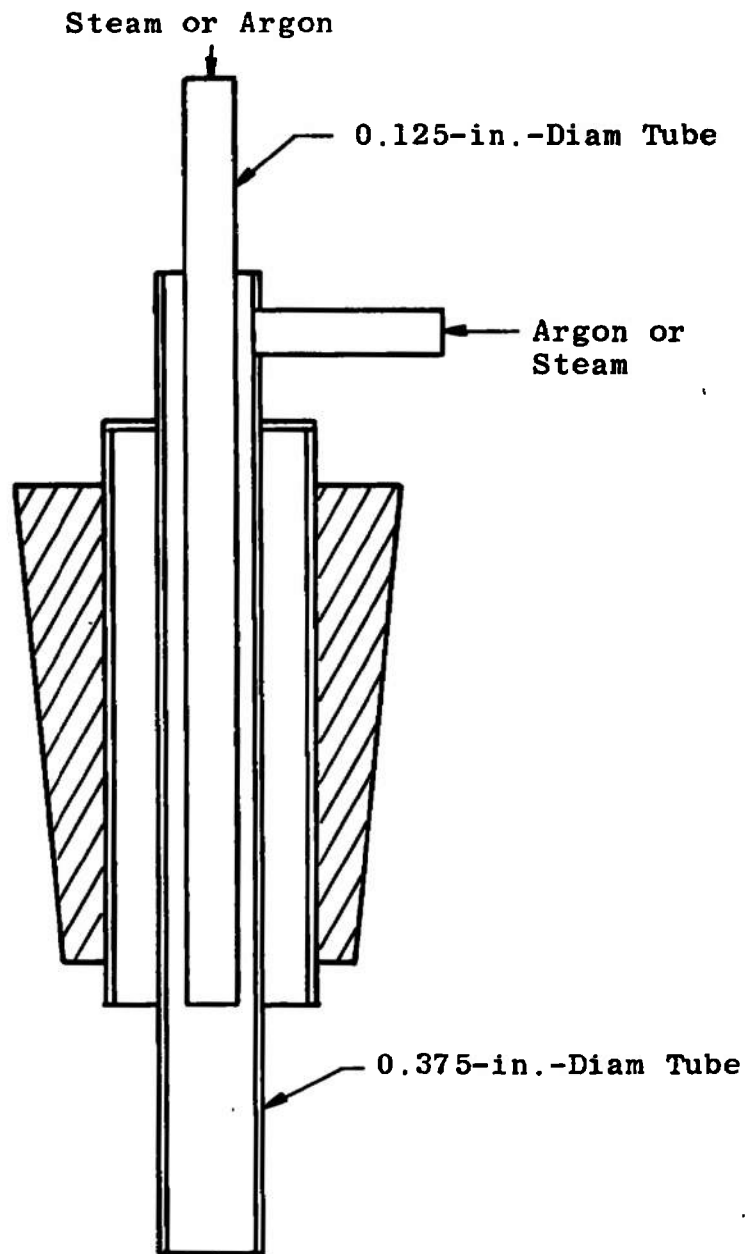
a. With Disc Electrodes
Fig. 8 Electrostatic Field Experiment Test Installation



b. With Sphere Electrodes
Fig. 8 Continued



c. Coaxial Nozzle with Sphere Electrodes
Fig. 8 Continued



d. Details of Coaxial Nozzle
Fig. 8 Concluded

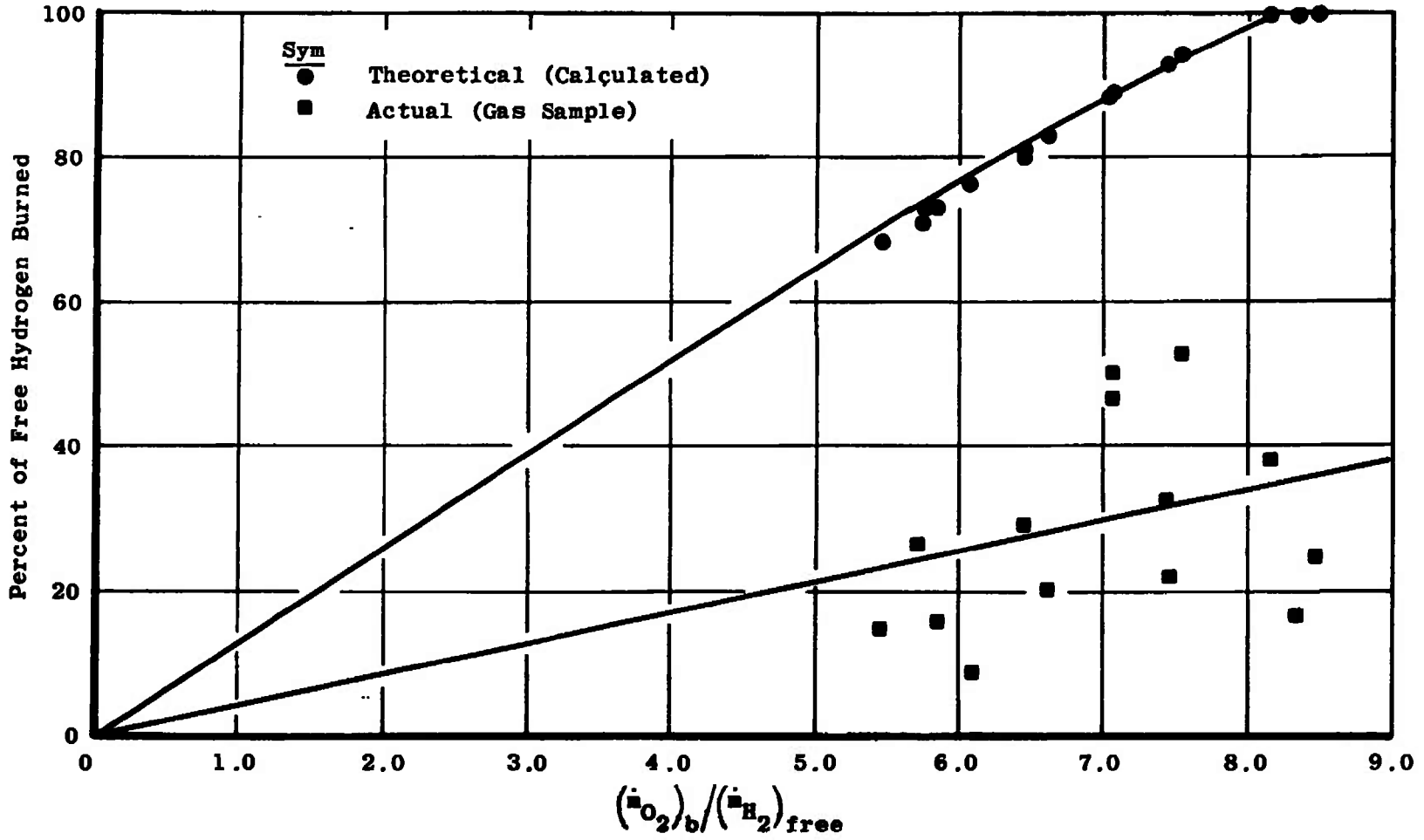


Fig. 9 Comparison of Theoretical and Actual (Gas Sample) Percent of Free Hydrogen Burned

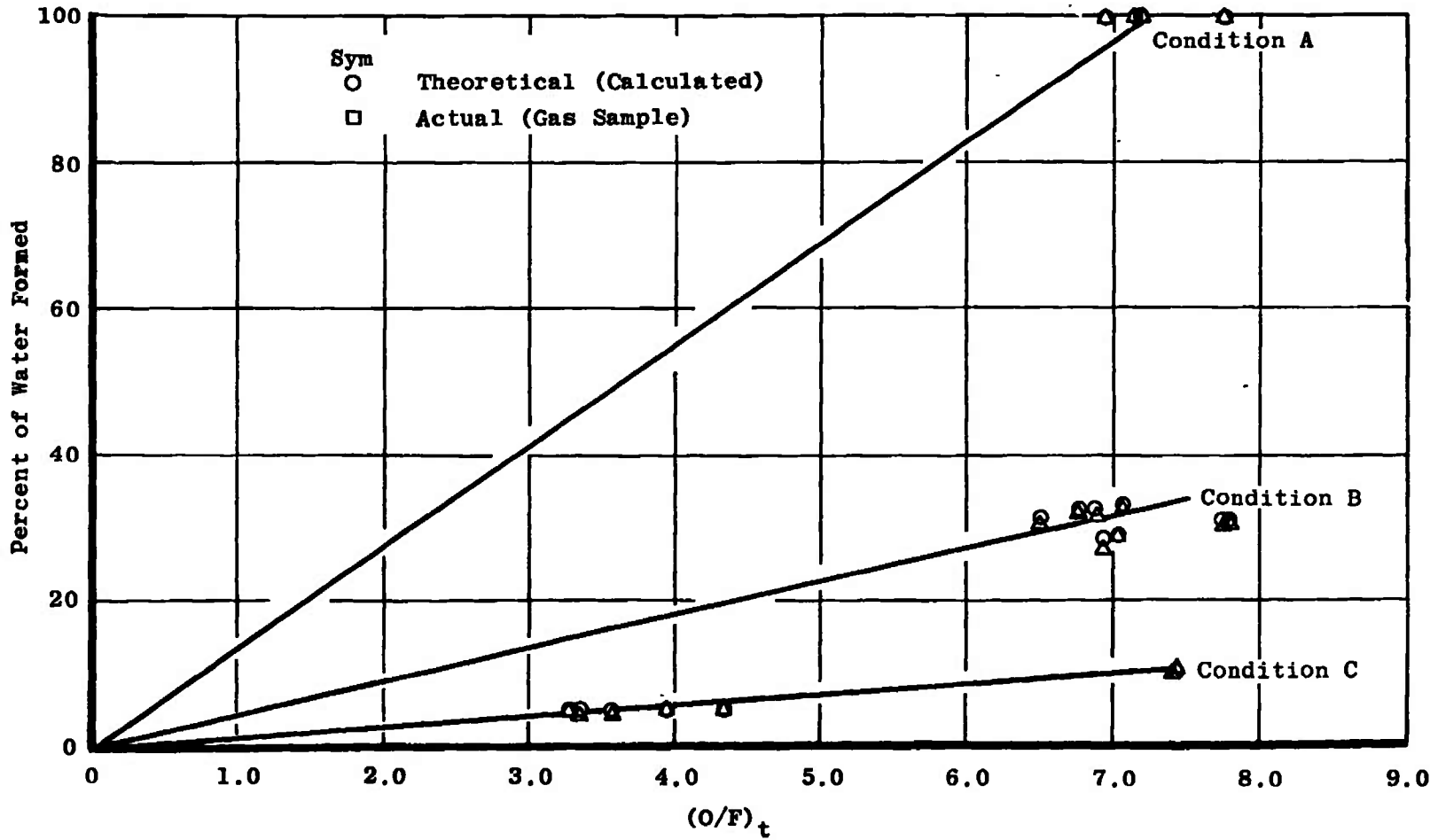


Fig. 10 Comparison of Theoretical and Actual (Gas Sample) Percent of Water Formed

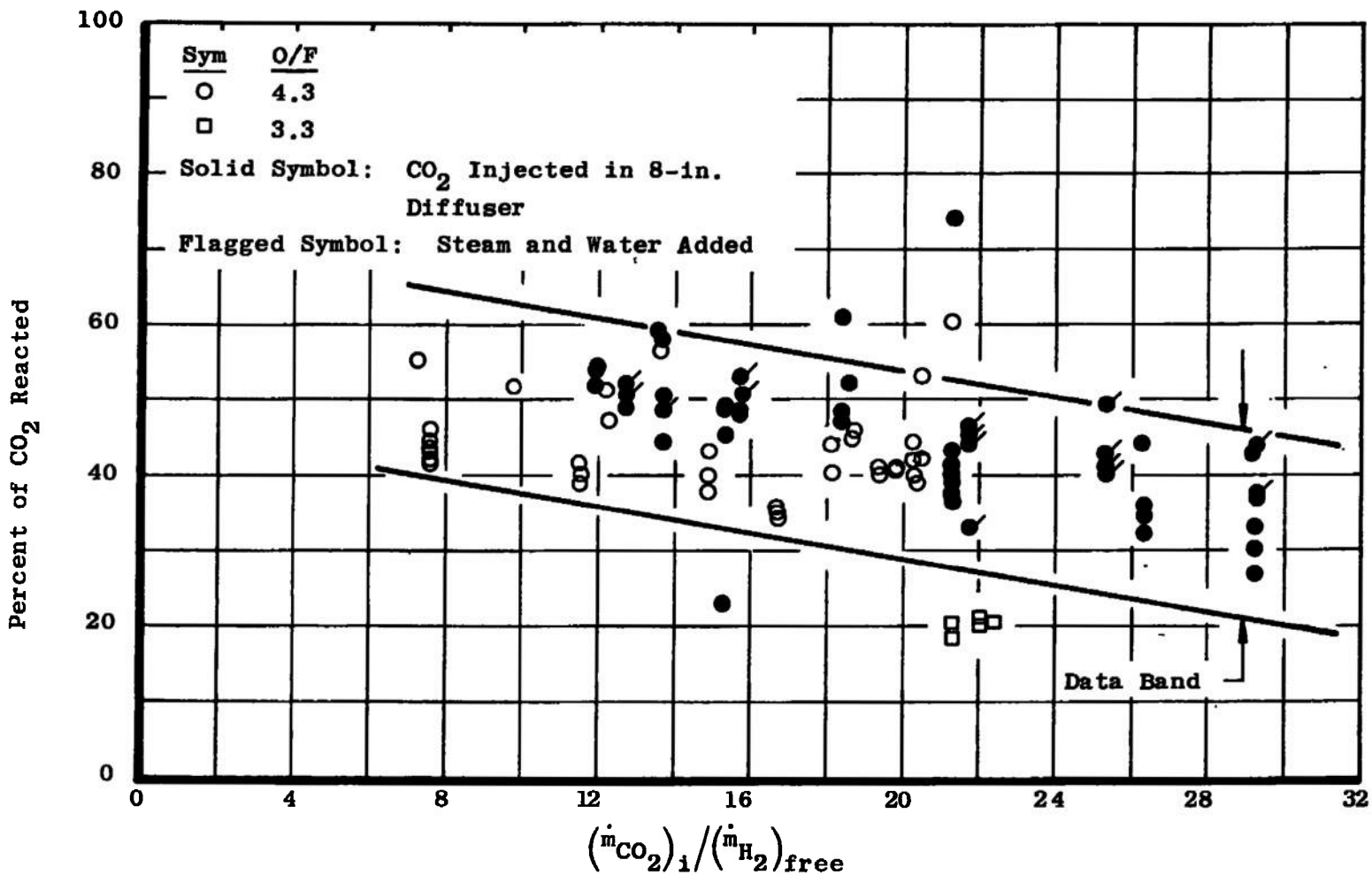


Fig. 11 Relation of Percent of Carbon Dioxide Reacted with Ratio of $(\dot{m}_{CO_2})_1 / (\dot{m}_{H_2})_{free}$

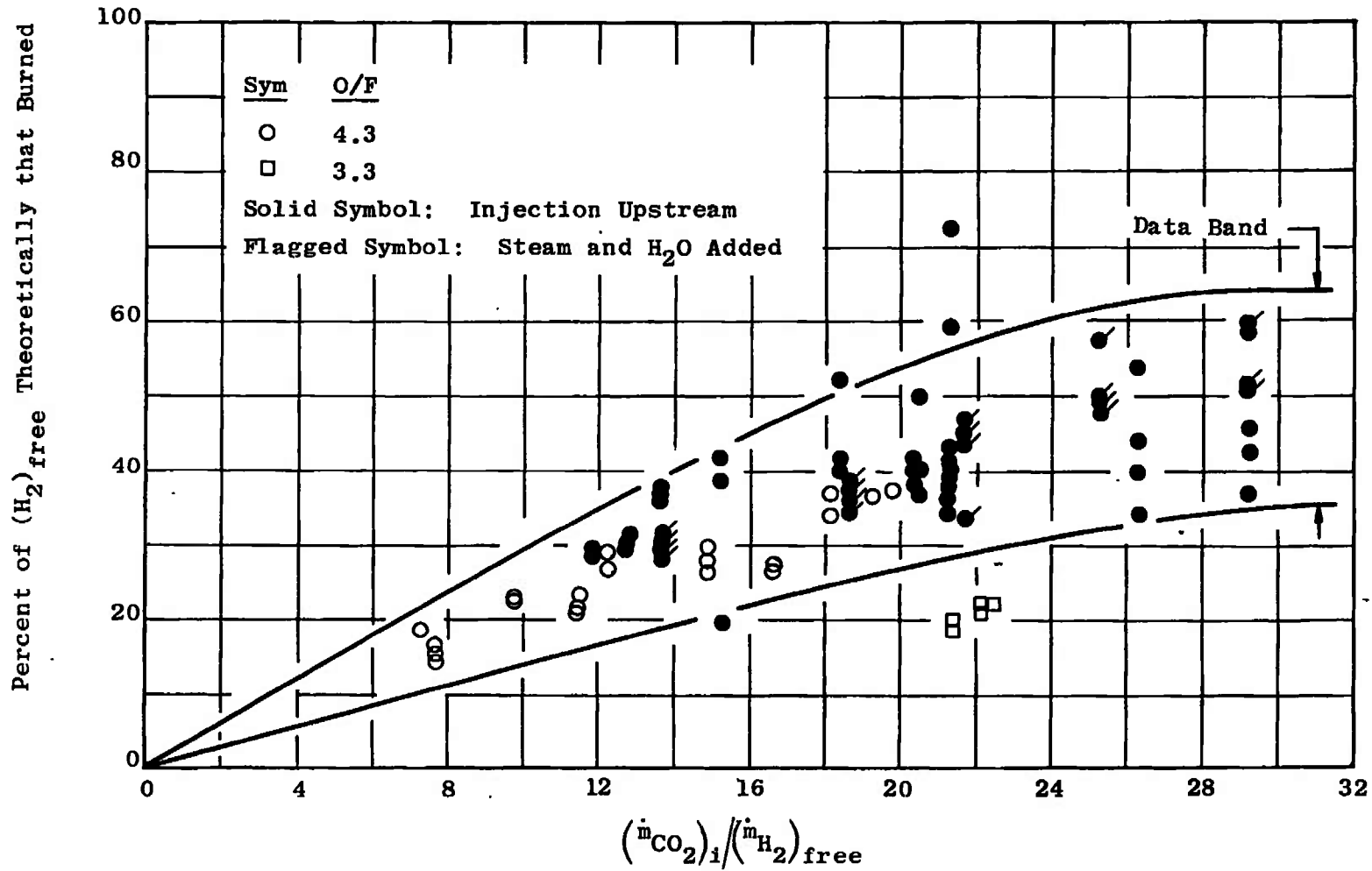


Fig. 12 The Theoretical Effect of Burning Free Hydrogen with Carbon Dioxide Injection

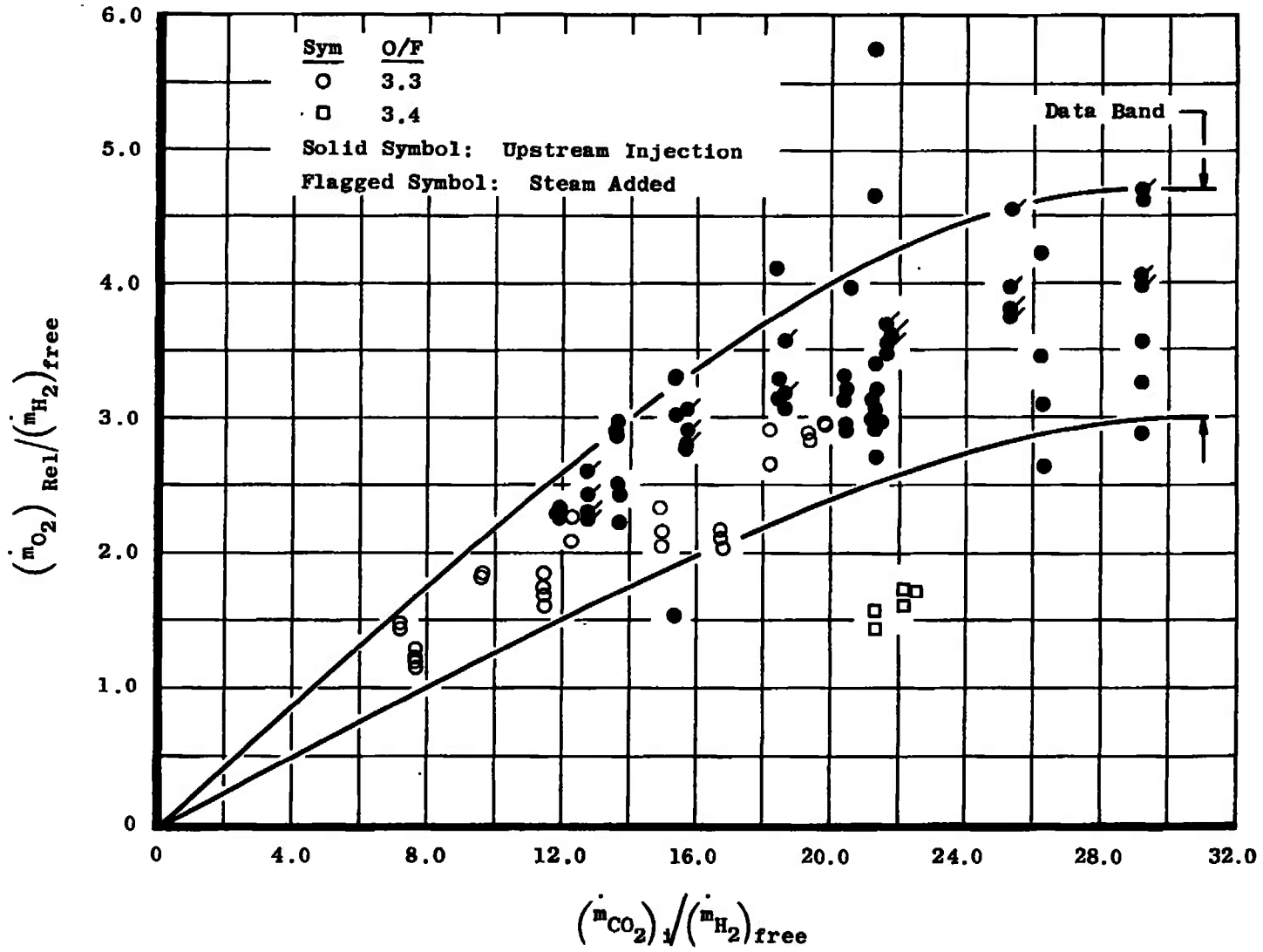


Fig. 13 Relation of Oxygen Released to the Carbon Dioxide Injected

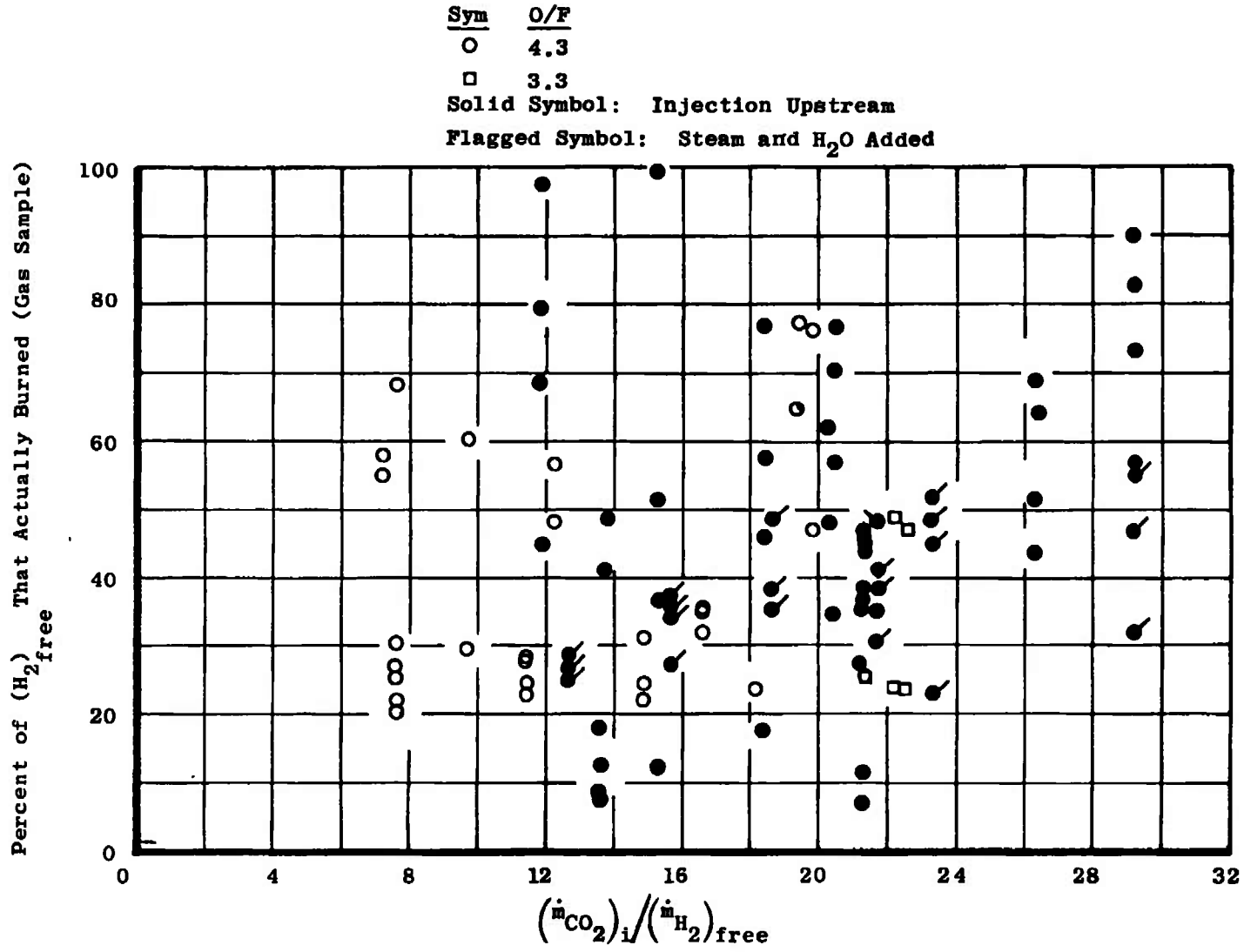


Fig. 14 The Actual (Gas Sample) Effect of Burning Free Hydrogen with Carbon Dioxide

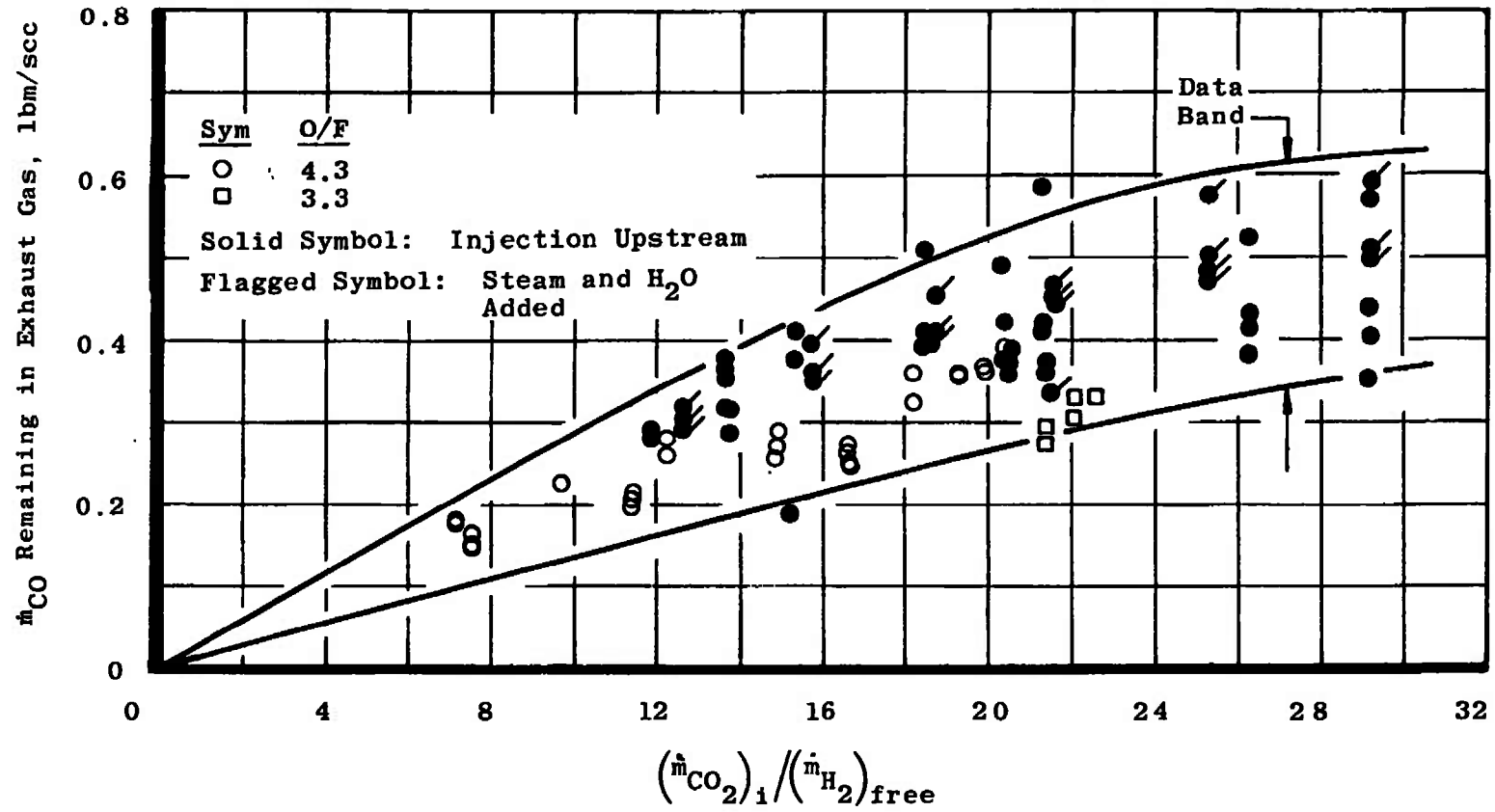


Fig. 15 Relation of Carbon Monoxide Remaining in the Exhaust Gas to the Ratio of $(\dot{m}_{CO_2})_i / (\dot{m}_{H_2})_{free}$

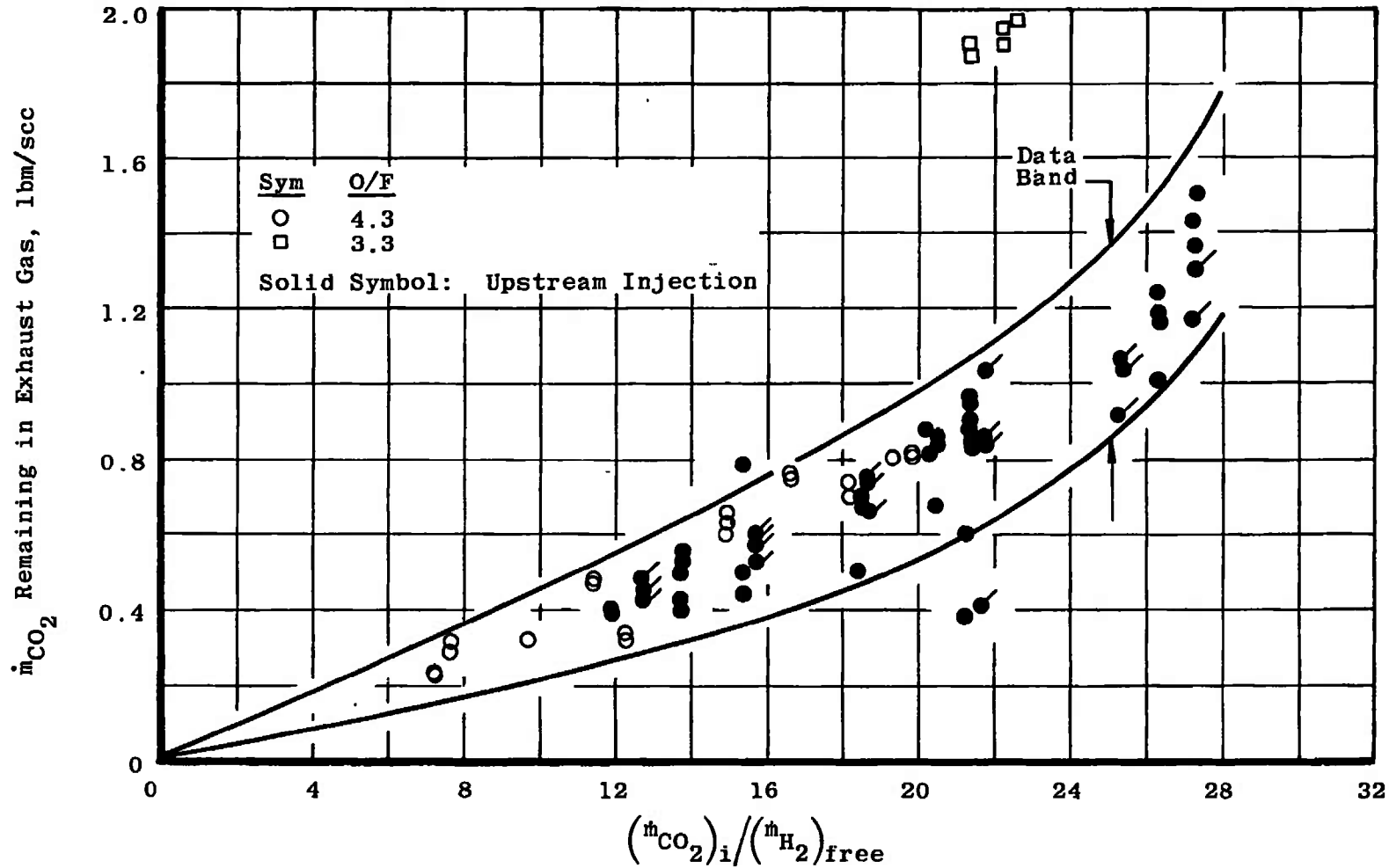


Fig. 16 Relation of Carbon Dioxide Remaining in the Exhaust Gas to the Ratio of $(\dot{m}_{CO_2})_i / (\dot{m}_{H_2})_{free}$

TABLE I
MEASUREMENT ACCURACY

Parameter	Range Measured	Instrument Full Range	Maximum Deviation
Engine O ₂ Pressure	500 to 575 psia	0 to 1000 psia	±0.17 psia
Engine H ₂ Pressure	375 to 500 psia	0 to 1000 psia	±0.06 psia
Manifold O ₂ Pressure	150 to 350 psia	0 to 1000 psia	±0.08 psia
Steam Pressure	30 to 40 psia	0 to 100 psia	±0.03 psia
P _t	240 to 260 psia	0 to 1000 psia	±0.16 psia
P _c	0.450 to 0.750 psia	0 to 2.00 psia	±0.006 psia
P _{ex}	0.900 to 2.000 psia	0 to 5.00 psia	±0.004 psia
Engine O ₂ Temperature	20 to 90°F	0 to 100°F	±2°F
Engine H ₂ Temperature	50 to 90°F	0 to 100°F	±2°F
Manifold O ₂ Temperature	50 to 90°F	0 to 100°F	±2°F
Steam Temperature	300 to 330°F	0 to 350°F	±7°F

TABLE II
SUMMARY OF OXYGEN INJECTION DATA

Data Point	Test No.	P _{cell} , psia	P _{ex} , psia	P _r , psia	mO ₂ , lbm/sec	mH ₂ , lbm/sec	m _{in} , lbm/sec	O/F	P _{ex} , psia	m _s , lbm/sec	(mO ₂) _b , lbm/sec	(mH ₂ O) _b , lbm/sec	(mH ₂) _{rec} , lbm/sec	(O/F) ₁	Percent Free H ₂ Burned	(mO ₂) _b / (mH ₂) _{rec}	mH ₂ O Formed, Burner, lbm/sec	mH ₂ O Total Formed, lbm/sec	mH ₂ O Formed, lbm/sec	Percent H ₂ O Formed (Theoretical)	Percent H ₂ O Formed (Gas Sample)	H ₂ O, Percent by Weight	H ₂ , Percent by Weight	mH ₂ O Flow, lbm/sec	mH ₂ Flow, lbm/sec	
1	HF-14	0.452	1.579	242	0.607	0.102	0.788	3.34	36.44	2.40	0	10	0.108	3.34	0	0	0	0.683	13.143	0.683	5.19	4.43	98.41	1.59	13.038	0.211
2	HF-15	---	---	243	0.598	0.182	0.780	3.28	37.23	2.52	0	10	0.107	3.29	0	0	0	0.873	13.193	0.673	5.10	4.81	88.60	1.11	13.152	0.148
4	↓	0.463	1.101	243	0.600	0.182	0.783	↓	36.44	2.46	0	↓	0.107	3.29	0	0	0	0.875	13.135	0.675	5.14	4.50	88.52	1.48	13.047	0.196
5	↓	0.467	1.199	244	0.601	0.183	0.784	↓	37.17	2.51	0.757	↓	0.108	7.44	88	7.044	0.852	1.528	14.039	0.877	10.89	10.80	99.59	0.41	13.904	0.058
6	↓	0.470	1.210	245	0.603	0.183	0.786	↓	37.28	2.52	0.764	↓	0.108	7.47	88	7.093	0.858	1.538	14.056	0.878	10.84	10.68	89.62	0.38	14.017	0.054
2	HF-18	0.482	0.987	245	0.613	0.171	0.784	3.58	37.57	2.53	0	10	0.084	3.56	0	0	0	0.689	13.218	0.689	5.21	4.12	88.09	1.91	13.069	0.255
3	↓	0.469	1.186	246	0.618	0.172	0.789	3.60	37.77	2.53	0.781	↓	0.085	6.14	100	8.268	0.879	1.574	14.014	0.885	11.16	10.76	88.58	0.41	14.083	0.058
4	↓	0.523	1.086	243	0.827	0.160	0.787	3.82	37.81	2.56	0	↓	0.082	3.82	0	0	0	0.705	13.265	0.705	5.32	5.05	88.11	0.89	13.228	0.118
5	↓	0.543	1.135	244	0.830	0.160	0.791	3.83	39.13	2.64	0.684	↓	0.082	8.19	100	8.375	0.770	1.478	14.039	0.708	10.53	10.02	98.52	0.48	14.047	0.068
2	HF-18	0.610	1.145	243	0.643	0.150	0.797	4.33	37.08	2.50	0	10	0.069	4.33	0	0	0	0.728	13.228	0.728	5.51	5.60	99.58	0.42	13.241	0.056
3	↓	0.734	1.175	244	0.654	0.150	0.804	4.36	36.56	2.47	0.580	10	0.068	8.22	100	8.493	0.654	1.388	13.857	0.735	10.01	8.66	99.63	0.37	13.803	0.051
2	HF-18	---	1.882	250	0.614	0.184	0.788	3.33	↓	↓	0.688	0	0.108	7.11	81	6.482	0.785	1.478	1.476	0.891	100	100	84.94	5.06	1.421	0.076
3	↓	---	1.878	252	0.620	0.187	0.806	3.32	↓	↓	0.722	0	0.108	7.10	83	6.610	0.813	1.508	1.509	0.887	100	100	94.30	5.70	1.442	0.087
4	↓	---	1.733	245	0.632	0.153	0.805	4.27	↓	↓	0.407	0	0.071	6.03	71	5.710	0.458	1.182	1.192	0.734	100	100	95.68	4.32	1.160	0.0524
5	↓	---	1.671	245	0.656	0.153	0.808	4.28	↓	↓	0.533	0	0.071	7.75	83	7.465	0.589	1.337	1.337	0.738	100	100	96.40	3.60	1.284	0.046
1	HF-20	0.507	---	244	0.602	0.183	0.785	3.29	36.44	2.95	0.657	0	0.108	6.88	76	8.098	0.738	1.417	4.367	0.678	32.44	31.48	97.79	2.21	4.305	0.097
2	↓	0.514	---	246	0.608	0.185	0.793	3.28	36.60	2.97	0.596	0	0.109	6.51	68	5.474	0.671	1.355	4.325	0.864	31.32	30.43	97.93	2.07	4.268	0.090
3	↓	0.523	---	240	0.637	0.152	0.789	4.19	36.37	2.85	0.413	0	0.072	6.01	71	5.708	0.464	1.182	4.132	0.717	28.61	26.73	87.63	2.17	4.062	0.090
4	↓	0.509	---	238	0.656	0.153	0.808	4.29	35.50	2.88	0.530	0	0.071	7.75	93	7.468	0.596	1.333	4.213	0.737	31.65	30.82	96.88	1.31	4.163	0.055
2	HF 21	---	1.845	255	0.623	0.187	0.811	3.33	---	2.85	0.704	0	0.109	7.09	80	8.435	0.782	1.494	4.444	0.701	33.61	32.04	97.22	2.76	4.341	0.124
3	↓	---	1.869	257	0.632	0.189	0.822	3.34	---	---	0.650	0	0.111	8.77	74	5.686	0.732	1.443	4.383	0.711	32.84	31.86	97.90	2.10	4.328	0.053
4	↓	---	1.758	248	0.683	0.152	0.815	4.38	---	---	0.403	0	0.088	7.02	73	5.835	0.453	1.198	4.149	0.748	28.88	28.19	98.58	1.42	4.108	0.085
5	↓	---	1.902	248	0.660	0.153	0.821	4.30	---	---	0.522	0	0.069	7.80	94	7.557	0.567	1.338	4.289	0.752	31.22	30.75	98.24	0.76	4.260	0.033

**TABLE III
SUMMARY OF CARBON DIOXIDE INJECTION DATA**

Test Number	Data Point	Probe						
		2	4	6	7	8	10	12
CO ₂ -2	5			X	X			
	6			X	X			
	7			X	X			
CO ₂ -3	3			X	X			
	4			X	X			
	5			X	X			
	6			X	X			
	7			X	X			
	8			X	X			
CO ₂ -4	1			X	X			
	2			X	X			
CO ₂ -5	2			X	X			
	3			X	X			
	4			X	X			
	5			X	X			
	6			X	X			
	7			X	X			
					X	X		
CO ₂ -6	1	X	X	X	X			
	2	X	X	X	X			
	3	X	X	X	X	X	X	X
	4	X	X	X	X			
	5	X	X	X	X			
	6	X	X	X	X			
CO ₂ -7	2	X	X	X	X			
	3	X	X	X	X			
	4	X	X	X	X	X	X	X
	5	X	X	X	X			
	6	X	X	X	X			
	7	X	X	X	X			
					X	X		

TABLE III (Continued)

Data Point	Test No.	\dot{m}_{O_2} lbm/sec	\dot{m}_{H_2} lbm/sec	\dot{m}_t lbm/sec	O/F	P_{t^*}	P_{ex^*}	$(\dot{m}_{CO_2})_i$ Injected, lbm/sec	$(\dot{m}_{H_2})_{free}$ lbm/sec	$(\dot{m}_{CO_2})_i / (\dot{m}_{H_2})_{free}$	\dot{m}_{H_2} Unburned, lbm/sec	\dot{m}_{CO} Formed, lbm/sec	\dot{m}_{CO_2} Not Reacted, lbm/sec	Percent H ₂ Burned	Percent CO ₂ Reacted	$(\dot{m}_{O_2})_{rel}$ Released from CO ₂ , lbm/sec	$\dot{m}_{CO} / (\dot{m}_{O_2})_{rel}$ Released	$(\dot{m}_{H_2})_{rel} / (\dot{m}_{H_2})_{free}$	Amount of $(\dot{m}_{H_2})_{free}$ Theoretical Burned, lbm/sec	Percent H ₂ Theoretical Burned	
4	CO ₂ -2	0.611	0.195	0.796	3.31	249	1.84	0	0.109	---	---	0	0	0	---	---	---	---	---	---	
5		0.612	0.189	0.799	3.30	248	1.91	2.33	0.110	21.2	0.065	0.273	1.902	41	18.4	0.155	1.765	1.420	0.019	0.178	
6		0.609	0.188	0.796	3.27	248	1.59	2.43	0.110	0.110	22.1	0.084	0.309	1.944	23.8	20.1	0.169	1.778	1.549	0.021	0.194
7	CO ₂ -3	0.608	0.186	0.794	3.26	248	1.60	2.50	0.110	22.7	0.055	0.334	1.911	49.8	21.4	0.207	1.512	1.885	0.028	0.236	
2		0.943	0.151	0.794	4.27	242	1.76	0	0.071	---	0	0	0	0	0.1	0.003	---	---	0.0004	0.0034	
3		0.648	0.152	0.800	4.27	244	1.67	1.28	0.071	18.0	0.021	0.328	0.793	70.3	40.4	0.191	1.711	2.686	0.024	0.336	
4		0.652	0.152	0.804	4.29	245	1.68	1.37	0.071	19.3	0.076	0.359	0.715	---	44.1	0.209	1.740	2.904	0.028	0.363	
5		0.653	0.152	0.805	4.28	245	1.88	1.40	0.070	20.0	0.015	0.356	0.807	78.5	41.1	0.207	1.725	2.910	0.028	0.364	
6		0.653	0.153	0.805	4.28	245	1.72	0.510	0.071	7.20	0.025	0.353	0.822	64.5	40.0	0.195	1.807	2.740	0.024	0.344	
7		0.653	0.153	0.806	4.28	245	1.74	0.690	0.071	9.7	0.017	0.363	0.930	75.9	40.7	0.207	1.754	2.957	0.026	0.370	
8		0.950	0.153	0.803	4.26	245	1.72	0.860	0.072	11.9	0.037	0.367	0.827	47.3	40.8	0.207	1.775	2.930	0.028	0.368	
1		CO ₂ -4	0.951	0.151	0.902	4.32	244	---	1.49	0.070	21.3	0.029	0.180	0.231	59.2	54.7	0.099	1.918	1.394	0.0124	0.174
2			0.657	0.152	0.808	4.33	246	---	1.48	0.070	21.2	0.032	0.183	0.226	55.4	55.7	0.101	1.801	1.428	0.0127	0.179
2	CO ₂ -5	0.648	0.152	0.800	4.26	244	1.4	1.48	0.071	20.56	0.028	0.225	0.330	90.1	51.3	0.128	1.788	1.803	0.016	0.225	
3		0.652	0.153	0.805	4.27	245	1.4	1.48	0.072	20.42	0.049	0.224	0.339	30.4	51.3	0.130	1.721	1.832	0.016	0.229	
4		0.641	0.153	0.784	4.19	243	1.4	1.48	0.073	20.30	0.030	0.257	0.453	58.9	47.3	0.150	1.722	2.076	0.019	0.260	
5		0.641	0.153	0.794	4.17	242	1.5	1.00	0.073	13.71	0.038	0.281	0.423	49.9	50.8	0.150	1.805	2.164	0.020	0.271	
											0.039	0.411	0.833	44.2	43.7	0.235	1.750	3.378	0.029	0.422	
										0.039	0.375	0.810	44.1	38.9	0.214	1.751	3.090	0.029	0.403		
										0.037	0.384	0.908	47.6	38.8	0.208	1.750	2.973	0.026	0.372		
										0.037	0.399	0.870	46.8	41.2	0.222	1.751	3.175	0.029	0.397		
										0.021	0.493	0.686	70.5	53	0.281	1.751	3.963	0.032	0.495		
										0.017	0.394	0.840	76.68	42	0.225	1.751	3.170	0.028	0.396		
										0.031	0.391	0.845	57.2	42	0.224	1.750	3.127	0.028	0.381		
										0.047	0.303	0.890	34.5	39	0.207	1.750	2.899	0.026	0.392		
										0.038	0.422	0.817	48.2	45	0.241	1.751	3.306	0.030	0.413		
										0.027	0.375	0.891	63	40	0.214	1.750	2.940	0.028	0.387		
										0.066	0.390	0.435	9.26	57	0.206	1.750	2.820	0.026	0.353		
										0.064	0.372	0.418	13.64	58	0.212	1.751	2.912	0.027	0.384		

TABLE III (Continued)

Data Point	Test No.	\dot{m}_{O_2} lbm/sec	\dot{m}_{H_2} lbm/sec	\dot{m}_f lbm/sec	O/F	P_{T^*}	P_{ex^*}	$(\dot{m}_{CO_2})_i$ Injected, lbm/sec	$(\dot{m}_{H_2})_{free}$ lbm/sec	$(\dot{m}_{CO_2})_i / (\dot{m}_{H_2})_{free}$	\dot{m}_{H_2} Unburned, lbm/sec	\dot{m}_{CO} Formed, lbm/sec	\dot{m}_{CO_2} Not Reacted, lbm/sec	Percent H_2 Burned	Percent CO_2 Reacted	$(\dot{m}_{O_2})_{rel}$ Released from CO_2 , lbm/sec	$\dot{m}_{CO} / (\dot{m}_{O_2})_{rel}$ Released	$(\dot{m}_{O_2})_{rel} / (\dot{m}_{H_2})_{free}$	Amount of $(\dot{m}_{H_2})_{free}$ Theoretical Burned, lbm/sec	Percent H_2 Theoretical Burned
8	CO ₂ -5	0.639	0.154	0.784	4.16	243	1.5	1.01	0.074	13.63	0.068	0.381	0.412	0.73	59	0.217	1.751	2.834	0.027	0.367
7		0.639	0.154	0.783	4.14	243	1.5	1.02	0.074	13.77	0.053	0.322	0.504	28.4	58	0.181	1.778	2.448	0.023	0.306
1	CO ₂ -6	0.642	0.151	0.783	4.26	243	0.886	2.065	0.071	28.08	0.044	0.288	0.566	40.87	45	0.185	1.751	2.228	0.021	0.278
2		0.646	0.151	0.787	4.28	243	1.041	1.848	0.070	28.40	0.038	0.316	0.524	48.6	48	0.181	1.750	2.436	0.023	0.305
3	0.645	0.152	0.797	4.24	243	1.146	1.528	0.071	21.54	0.030	0.570	1.170	57.28	43.34	0.326	1.754	4.577	0.041	57.2	
4										0.007	0.356	1.506	90.00	27.07	0.203	1.754	2.869	0.025	35.8	
5	0.642	0.152	0.785	4.22	242	1.252	1.321	0.072	18.34	0.019	0.440	1.374	73.5	33.48	0.251	1.753	3.535	0.031	44.2	
6										0.012	0.403	1.432	82.8	30.65	0.230	1.752	3.238	0.028	40.4	
7	0.642	0.152	0.785	4.22	243	1.323	0.857	0.072	11.90	0.025	0.425	1.180	64.0	38.15	0.243	1.749	3.471	0.030	43.4	
8										0.034	0.521	1.030	51.0	44.28	0.297	1.754	4.243	0.037	53.0	
9	0.642	0.152	0.785	4.22	243	1.323	0.857	0.072	11.90	0.021	0.381	1.248	69.6	32.47	0.218	1.752	3.114	0.027	39.0	
10										0.038	0.413	1.188	44.0	35.12	0.236	1.750	3.371	0.030	42.1	
11	0.642	0.152	0.785	4.22	243	1.323	0.857	0.072	11.90	0.045	0.587	0.807	36.6	60.30	0.335	1.752	4.718	0.042	58.0	
12										0.044	0.406	0.892	38.2	41.66	0.231	1.759	3.254	0.029	40.7	
13	0.642	0.152	0.785	4.22	243	1.323	0.857	0.072	11.90	0.053	0.720	0.387	27.5	77.31	0.412	1.748	5.803	0.052	72.5	
14										0.039	0.388	0.888	46.1	47.08	0.226	1.752	3.138	0.028	38.3	
15	0.642	0.152	0.785	4.22	243	1.323	0.857	0.072	11.90	0.017	0.411	0.875	76.6	48.90	0.235	1.748	3.284	0.029	40.8	
16										0.031	0.411	0.875	57.7	48.80	0.235	1.748	3.284	0.028	40.8	
17	0.642	0.152	0.785	4.22	243	1.323	0.857	0.072	11.90	0.058	0.514	0.513	18.4	61.17	0.284	1.748	4.083	0.037	51	
18										0.052	0.194	0.785	12.5	27.73	0.111	1.748	1.563	0.014	19.6	
19	0.642	0.152	0.785	4.22	243	1.323	0.857	0.072	11.90	0.034	0.380	0.503	51.8	54.27	0.217	1.751	3.056	0.027	38.2	
20										0.0002	0.413	0.451	88.8	59.00	0.236	1.750	3.324	0.030	41.5	
21	0.642	0.152	0.785	4.22	243	1.323	0.857	0.072	11.90	0.045	0.453	0.453	38.5	58.82	0.238	1.742	3.324	0.030	41.5	
22										0.002	0.295	0.394	87.1	54.03	0.168	1.756	2.333	0.021	29.2	
23	0.642	0.152	0.785	4.22	243	1.323	0.857	0.072	11.90	0.040	0.292	0.387	45.0	53.68	0.168	1.738	2.333	0.021	28.2	
24										0.023	0.288	0.405	88.7	52.74	0.164	1.756	2.278	0.021	28.5	
25	0.642	0.152	0.785	4.22	243	1.323	0.857	0.072	11.90	0.015	0.295	0.383	79.8	54.14	0.167	1.746	2.347	0.021	29.3	

TABLE III (Concluded)

Data Point	Test No.	\dot{m}_{O_2} lbm/sec	\dot{m}_{H_2} lbm/sec	\dot{m}_f lbm/sec	O/F	P_{T_1}	P_{ex}	$(\dot{m}_{CO_2})_1$ Injected, lbm/sec	$(\dot{m}_{H_2})_{free}$ lbm/sec	$(\dot{m}_{CO_2})_1 / (\dot{m}_{H_2})_{free}$	\dot{m}_{H_2} Unburned, lbm/sec	\dot{m}_{CO} Formed, lbm/sec	\dot{m}_{CO_2} Not Reacted, lbm/sec	Percent H_2 Burned	Percent CO_2 Reacted	$(\dot{m}_{O_2})_{rel}$ Released from CO_2 , lbm/sec	$\dot{m}_{CO} / (\dot{m}_{O_2})_{rel}$ Released	$(\dot{m}_{H_2})_{rel} / (\dot{m}_{H_2})_{free}$	Amount of $(\dot{m}_{H_2})_{free}$ Theoretical Burned, lbm/sec	Percent H_2 Theoretical Burned
2	CO ₂ -7	0.641	0.153	0.794	4.20	242		2.10	0.072	29.25	0.049	0.590	1.173	32.08	44.15	0.337	1.751	4.895	0.042	59.2
											0.032	0.497	1.319	55.20	37.21	0.284	1.750	3.957	0.038	49.9
											0.038	0.506	1.305	47.44	37.87	0.289	1.751	4.026	0.036	50.7
3		0.645	0.153	0.799	4.207	244		1.827	0.072	25.34	0.035	0.479	1.074	51.88	41.19	0.274	1.751	3.795	0.034	47.8
											0.040	0.574	0.925	45.02	49.39	0.328	1.751	4.549	0.041	57.3
											0.055	0.500	1.041	23.23	43.03	0.256	1.751	3.964	0.036	49.9
											0.037	0.472	1.085	48.73	40.81	0.270	1.750	3.741	0.034	47.1
											0.042	0.441	0.879	41.83	44.07	0.252	1.751	3.481	0.032	43.9
											0.080	0.729	0.928	-10.03	72.82	0.418	1.751	5.751	0.052	72.5
4		0.848	0.154	0.789	4.199	244		1.573	0.072	21.73	0.050	0.448	0.869	30.44	44.74	0.256	1.750	3.535	0.032	44.5
											0.050	0.467	0.840	30.70	48.63	0.267	1.751	3.802	0.034	46.4
											0.138	0.336	1.045	-87.30	33.54	0.192	1.751	2.649	0.024	33.4
											0.123	0.451	0.864	-70.17	45.09	0.258	1.751	3.561	0.032	44.9
											0.277	0.445	0.874	-282.8	44.44	0.254	1.751	3.510	0.032	44.2
											0.038	0.396	0.749	48.59	45.38	0.226	1.751	3.078	0.029	38.8
5		0.641	0.154	0.795	4.155	243		1.371	0.074	18.85	0.045	0.459	0.650	38.26	52.60	0.262	1.750	3.567	0.033	44.9
											0.048	0.408	0.730	35.43	46.75	0.233	1.751	3.170	0.029	39.9
											0.046	0.359	0.594	37.44	48.72	0.205	1.751	2.786	0.026	35.1
6		0.641	0.155	0.798	4.150	243		1.159	0.074	15.73	0.049	0.394	0.540	34.14	53.43	0.225	1.751	3.054	0.028	38.5
											0.053	0.371	0.575	27.75	50.35	0.212	1.750	2.879	0.027	36.3
											0.047	0.358	0.800	36.49	48.19	0.203	1.750	2.754	0.026	34.7
											0.056	0.298	0.479	24.73	49.40	0.170	1.750	2.289	0.021	20.8
											0.055	0.296	0.482	25.72	49.09	0.169	1.751	2.275	0.021	28.7
7		0.630	0.155	0.794	4.187	243		0.947	0.074	12.75	0.053	0.315	0.452	27.91	52.24	0.180	1.751	2.420	0.023	30.5
											0.054	0.305	0.967	26.69	50.64	0.174	1.750	2.347	0.022	29.6

APPENDIX III GAS SAMPLE ANALYSIS CALCULATION

The results of the gas sample analysis obtained from the laboratory were presented in percent by volume of H₂, O₂, and N₂. The H₂O was shown in milligrams.

The molecular weight [(mole wt)_{mix}] of the mixture is

$$\begin{aligned} & (\% \text{ by vol})_{\text{H}_2} (\text{mole wt})_{\text{H}_2} + (\% \text{ by vol})_{\text{O}_2} (\text{mole wt})_{\text{O}_2} \\ & + (\% \text{ by vol})_{\text{N}_2} (\text{mole wt})_{\text{N}_2} + (\% \text{ by vol})_{\text{H}_2\text{O}} (\text{mole wt})_{\text{H}_2\text{O}} \end{aligned}$$

The gas constant of the mixture is

$$R_{\text{mix}} = \frac{1545}{(\text{mole wt})_{\text{mix}}}$$

The original sample bottle contained H₂O (gas), N₂, O₂, H₂ and H₂O (liquid). The temperature of the mixture (T_{mix}) and volume of the sample bottle were known. The pressure of the mixture (p_{mix}) of the original bottle was not known. The original samples were divided into sample bottles 1 (the original bottle) and 2. Sample bottle 1 contained H₂O (gas), N₂, O₂, H₂, and H₂O (liquid). Sample bottle 2 contained the same gaseous constituents but no liquid H₂O. In both bottles 1 and 2, the pressure, temperature, and volume were known.

If it is assumed that the liquid water volume in bottle 1 is small compared with the container volume and if the perfect gas equation for gases is used,

$$pV = mRT$$

then

$$m_{\text{mix}} = \frac{p_{\text{mix}} V_{\text{mix}}}{R_{\text{mix}} T_{\text{mix}}}$$

$$m_1 = \frac{p_1 V_1}{R_{\text{mix}} T_{\text{mix}}}$$

and

$$m_2 = \frac{p_2 V_2}{R_{\text{mix}} T_{\text{mix}}}$$

but

$$m_{\text{mix}} = m_1 + m_2 + m_{\text{H}_2\text{O}} (\text{liquid})$$

or this equals the total mass in the original sample bottle.

$$m_{\text{mix(gas)}} = m_1 + m_2$$

This includes the mass of water vapor in the sample. The constituents in the original gas sample can be shown as

$$m_{\text{H}_2\text{O(gas)}} = (\% \text{ by wt}) (m_{\text{mix(gas)}})$$

$$m_{\text{H}_2} = (\% \text{ by wt}) (m_{\text{mix(gas)}})$$

$$m_{\text{O}_2} = (\% \text{ by wt}) (m_{\text{mix(gas)}})$$

$$m_{\text{N}_2} = (\% \text{ by wt}) (m_{\text{mix(gas)}})$$

$$m_{\text{H}_2\text{O}} = m_{\text{H}_2\text{O(liquid)}} + m_{\text{H}_2\text{O(gas)}}$$

$$m_{\text{sample}} = m_{\text{mix(gas)}} + m_{\text{H}_2\text{O(liquid)}}$$

which equals to

$$m_{\text{H}_2\text{O}} + m_{\text{H}_2} + m_{\text{N}_2} + m_{\text{O}_2}$$

where $m_{\text{H}_2\text{O}}$ includes both liquid and gaseous water as indicated above.

The percent by weight of the gases and water as analyzed from the sample is shown as

$$\% \text{ by wt H}_2\text{O} = \frac{(m_{\text{H}_2\text{O}}) (100)}{m_{\text{sample}}}$$

$$\% \text{ by wt H}_2 = \frac{(m_{\text{H}_2}) (100)}{m_{\text{sample}}}$$

$$\% \text{ by wt O}_2 = \frac{(m_{\text{O}_2}) (100)}{m_{\text{sample}}}$$

$$\% \text{ by wt N}_2 = \frac{(m_{\text{N}_2}) (100)}{m_{\text{sample}}}$$

The presence of N_2 in the sample had to come from air leakage in the ducting or sampling system. From the data, the percent by weight of the O_2 was equal to or less than the ratio of O_2 to N_2 found in the air; therefore the sample of gas with the air removed contains only H_2 and H_2O . Thus

$$m_{\text{O}_2} = (\% \text{ by wt}) (m_{\text{mix(gas)}}) - (1/3) m_{\text{N}_2}$$

APPENDIX IV VENTURI MASS FLOW EQUATION FOR GASEOUS CARBON DIOXIDE

Because the thermodynamic properties of CO₂ deviate considerably from the perfect gas values, the derivation of a venturi mass flow equation for CO₂ was considered necessary. When the approach velocity is not zero, the complete mass flow (as shown in Standards for Steam Jet Ejectors¹) is

$$\dot{m} = \sqrt{\frac{2g_c}{R}} A_2 \sqrt{\frac{p_1 \Delta p}{T_1}} \frac{y_a}{\sqrt{1-\beta^4}} C_D$$

where

$$A_2 = \frac{\pi}{4} (0.499)^2 = 0.19556 \text{ in.}^2$$

p_1 = upstream venturi pressure, psia

p_2 = venturi throat pressure, psia

Δp = $p_1 - p_2$, psia

g_c = 32.174 ft-lbm/lbf-sec²

R = 35.11 ft-lbf/lbm-°R

T_1 = °R

C_D = 1.0

β = 0.499/0.8 = 0.62375 = ratio of venturi throat diameter to pipe diameter (d_2/d_1)

The expansion factor is y_a :

$$y_a = \left[(r)^{2/\gamma} \left(\frac{\gamma}{\gamma-1} \right) \left(\frac{1-(r)^{\frac{\gamma-1}{\gamma}}}{1-r} \right) \left(\frac{1-\beta^4}{1-\beta^4 (r)^{2/\gamma}} \right) \right]^{\frac{\gamma}{\gamma-1}}$$

where

$$y = 1.5$$

then

$$y_a = \left[r^{1.333} \left(\frac{1-r^{0.333}}{1-r} \right) \left(\frac{2.546}{1-(0.1514)r^{1.333}} \right) \right]^{\frac{1.5}{0.5}}$$

¹"Standards for Steam Jet Ejectors." Third Edition. Heat Exchange Institute, New York 17, New York, 1956.

$$\dot{m} = \sqrt{\frac{(2)(32.174)}{35.11}} (0.19556) \frac{(1.0)}{0.92121} y_a \sqrt{\frac{p_1 \Delta p}{T_1}}$$

$$\dot{m} = (0.2874) \left[\frac{p_1^2 (1-r)}{T_1} r^{1.333} \left(\frac{1-r^{0.333}}{1-r} \right) \left(\frac{2.546}{1-(0.1514)r^{1.333}} \right) \right]^{1/2}$$

by reducing the above equations to the usable form,

$$\dot{m} = 0.4568 \left[\frac{p_1^2 r^{1.333}}{T_1} \frac{1-r^{0.333}}{1-(0.1514)r^{1.333}} \right]^{1/2}$$

where

$$r = p_2/p_1$$

UNCLASSIFIED

Security Classification

14. KEY WORDS	LINK A		LINK B		LINK C	
	ROLE	WT	ROLE	WT	ROLE	WT
performance evaluation altitude test facilities improvement exhaust systems combustion products contaminants exhaust gases toxicology hazardous materials gas scrubbing electrostatic field						

[Handwritten scribbles and illegible text]